Electronic Supplementary Material (ESI) for Journal of Materials Chemistry B.

Supporting Information for

Divergent Approach to Nanoscale Glycomicelles and Photo-Responsive Supramolecular Glycogels. Implications for Drug Delivery and Photoswitching Lectin Affinity

Elena Romero-Ben[1], Mª Carmen Castillejos[1], Cristian Rosales-Barrios[1], María Expósito[1], Pilar Ruda[1], Paula M. Castillo,[1] Stefania Nardecchia,[2] Juan de Vicente,[2] Noureddine Khiar.*[1]

[1]Asymmetric Synthesis and Functional Nanosystem Group. Institute of Chemical Research (IIQ), CSIC-University of Seville. Avda. Américo Vespucio 49, 41092, Seville. Spain.
E-mail: khiar@iiq.csic.es.

[2]Department of Applied Physics and Excellence Research Unit 'Modeling Nature' (MNat),

Faculty of Sciences, University of Granada, C/Fuentenueva s/n, 18071 - Granada, Spain

TABLE OF CONTENTS

1. Synthesis of Bifunctional Spacers 7-9

1.1. Synthesis of TEG-derived bifunctional **7**

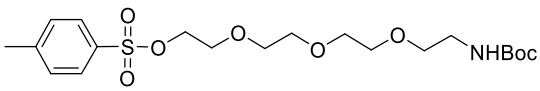

To a solution of 2-[2-[2-(2-Azidoethoxy)ethoxy]ethoxy]ethanol (0.02 M, 1 eq) in CH_2Cl_2 was added Pd/C (0.1 equiv.). Subsequently, the reaction was placed under hydrogen pressure (4 bars), and stirred for 24 hours. Then, the reaction mixture was filtered over Celite® and purified by column chromatography using CH_2Cl_2 / MeOH (9 : 1) as eluent affording 2-[2-[2-(2-Aminoethoxy)ethoxy]ethoxy]ethanol with a 90% yield. Next, to a solution of the obtained amine (100 mg, 0.517 mmol) in tetrahydrofuran (THF) (0.83 mL), was added dropwise ditertbutyl dicarbonate (0.42 mL, 1.86 mmol), and the reaction mixture was stirred under argon atmosphere for 1 hour. After evaporation of the solvent, the crude product was purified by column chromatography (CH_2Cl_2 / MeOH (15 : 1)), affording 1-Boc-amino-etraethylene glycol as a yellow syrup with 91% yield. Next, a solution of *p*-toluenesulfonyl chloride (1.1 g, 5.79 mmol) in THF (1.6 mL) was added dropwise to a solution of 1-Boc-amino-etraethylene glycol (1.7 g, 5.79 mmol) and Et_3N (0.49 mL) in THF (1.6 mL) at 0˚C, and the reaction mixture was stirred overnight at room temperature. The reaction mixture was filtered over celite®, washed with ethyl acetate (AcOEt) and purified by column chromatography (AcOEt / Hexane (2 : 1)), affording spacer **7** as a yellow syrup with 42% yield. R*f* : 0.343. AcOEt / Hexane (1 : 1). ^{1}H NMR (400 MHz, $CDCl_3$): δ 7.77 (d, 2H, *J* = 8.25 Hz), 7.32 (d, 2H, *J* = 8.12 Hz), 5.28 (s, 1H), 4.14 (t, 2H, *J* = 4.75 Hz), 3.67 (t, 2H, *J* = 4.92 Hz), 3.61-3.56 (m, 8H), 3.50 (t, 2H, *J* = 5.08 Hz), 3.27 (t, 2H, *J* = 4.98 Hz), 2.42 (s, 3H), 1.41 (s, 9H). ^{13}C NMR (100 MHz, $CDCl_3$): δ 155.9, 144.8, 132.9, 129.8, 127.9, 79.1, 70.7-69.2 (m), 68.6, 40.5, 28.4, 21.6. HRMS: Calcd. for $C_{20}H_{33}O_8SNNa$: 470.1819 [M+Na]+, found: 470.1815.

1.2. Synthesis of TEG derived bifunctional spacer **8**

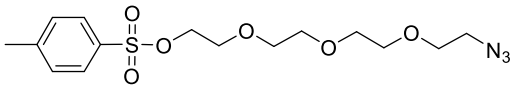

To a solution of 2-[2-[2-(2-Azidoethoxy)ethoxy]ethoxy]ethanol (3 g, 0.013 mmol) in THF (6 mL) and Et_3N (0.87 mL), was added dropwise a solution *p*-toluenesulfonyl chloride (2.47 mg, 0.013 mmol) in THF (2 mL) at 0˚C. The reaction was then allowed to reach room temperature, and stirred overnight. The reaction mixture was filtered over celite®, washed with AcOEt and evaporated. Finally, the crude product was purified by column chromatographic (AcOEt / Hexane (1: 1)), affording the desired compound **8** as a yellow syrup with a 40% isolated yield. R*f*: 0.447 AcOEt/Hexano (1:1). ^{1}H RMN (400MHz, $CDCl_3$): δ 7.81 (d, 2H, *J* = 7,67Hz), 7,36 (d, 2H, J = 7,29Hz), 4,18 (t, 2H, J=4,55Hz, -SOO-O-C$\underline{H_2}$-), 3,75-3,55 (m, 12H, 6 OCH_2), 3,39 (t, 2H, J=4,7Hz, CH_2-N_3), 2,46 (s, 3H, Ar-C$\underline{H_3}$). ^{13}C RMN (100MHz, $CDCl_3$): δ 144,6 (C-Ar), 132,9 (C-Ar), 129,8 (2CH-Ar), 127,9 (2CH-Ar), 70,6-69,3 (CH_2O-), 68,6 (-SO_3CH_2-), 50,6 (CH_2N_3), 21,6 (C-$\underline{C}H_3$). HRMS: Calcd. for $C_{15}H_{23}O_6N_3SNa$ 396.1200 $[M+Na]^+$, found 396.1193

1.3. Synthesis of PEG20-derived bifunctional spacer **9**

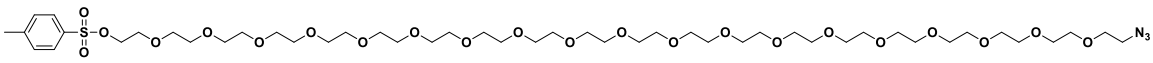

To a mixture of N_3-PEG_{20}-OH (600 mg, 0,65 mmol) in THF (1 mL) and Et_3N (0,043 mL) was added dropwise at 0ºC, a solution *p*-toluenesulfonyl chloride (124 mg, 0,65 mmol) in THF (0,3 mL). The reaction was then allowed to reach room temperature, and stirred overnight. The reaction mixture was filtered over celite®, washed with AcOEt and evaporated. The crude mixture was purified by flash column chromatographic (CH_2Cl_2 / MeOH from 30 : 1 to 10 : 1)), affording compound **9** as a white solid in 67% isolated yield. R*f*: 0.54 CH_2Cl_2 / MeOH (20:1). ^{1}H NMR (400MHz, $CDCl_3$): δ 7.81 (d, 2H, J=7.95Hz, Ar), 7.36 (d, 2H, J=7.95Hz, Ar), 4.18 (t, 2H, J=3.67Hz, SOOOC$\underline{H_2}$), 3.75-3.45 (m, 76H, 38 O$\underline{CH_2}$), 3.41 (t, 2H, J = 4.70Hz, C$\underline{H_2}$-N_3), 2.65 (s, 3H, Ar-C$\underline{H_3}$). ^{13}C NMR (100MHz, $CDCl_3$): δ 144.8 (C-Ar), 133.0 (C-Ar), 129.9 (2CH-Ar), 128.0 (2CH-Ar), 70.6 (36CH_2O-), 70.1 (CH_2O-), 69.3 (SOOO$\underline{C}H_2$), 68.2 (CH_2O), 50.7 (CH_2N_3), 21.7 (C-$\underline{C}H_3$). HRMS: Calcd. for $C_{47}H_{87}O_{22}N_3NaS$ a 1100.5394 $[M+Na]^+$, found 1100.5394.

2. ^{1}H AND ^{13}C NMR SPECTRA

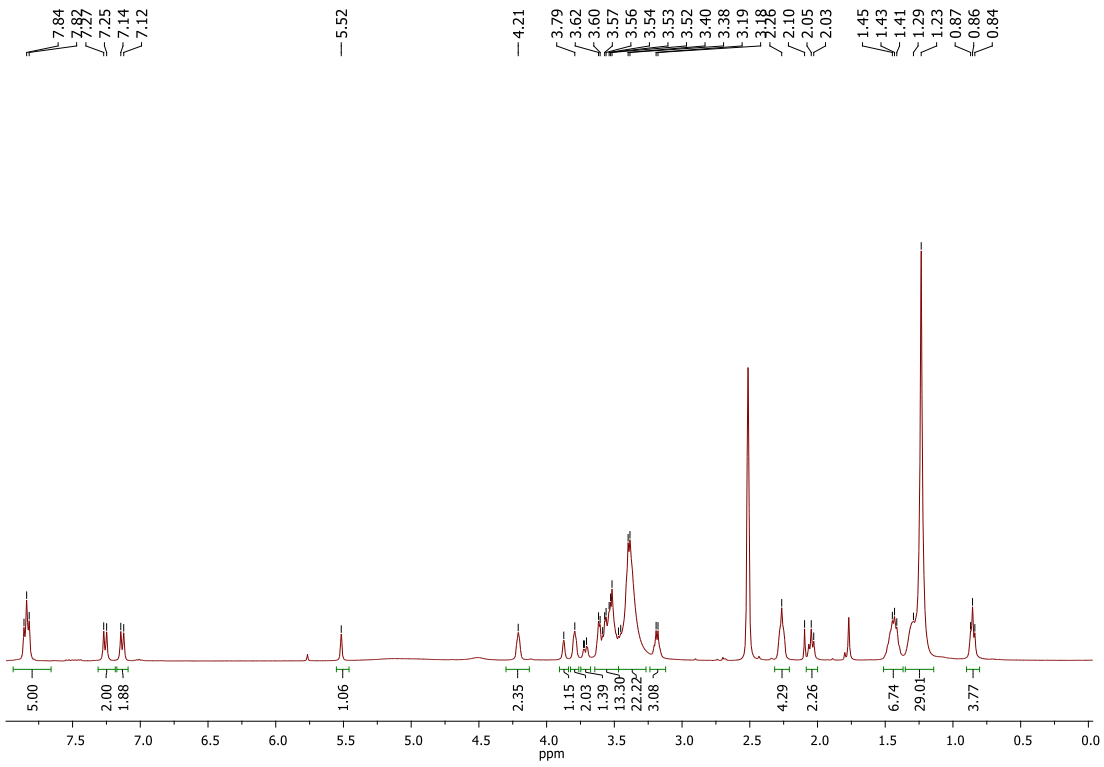

Figure S1. ^{1}H NMR of compound **1** in DMSOd_6

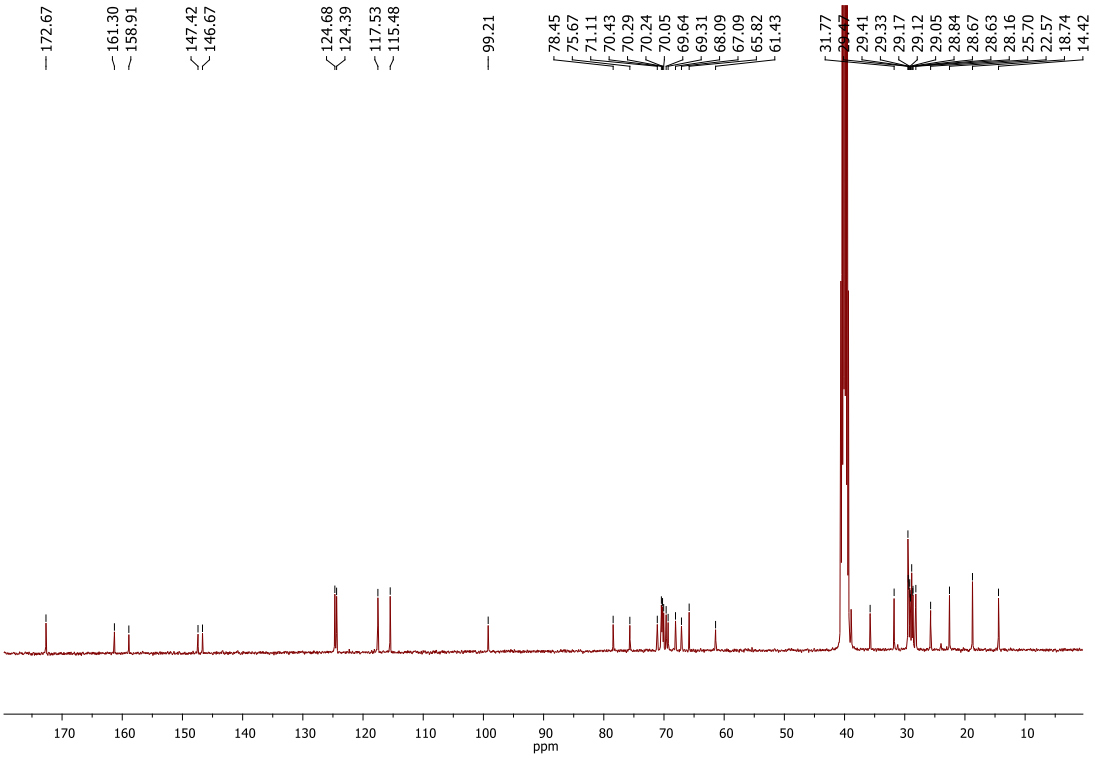

Figure S2. ^{13}C NMR of compound **1** in $DMSOd_6$

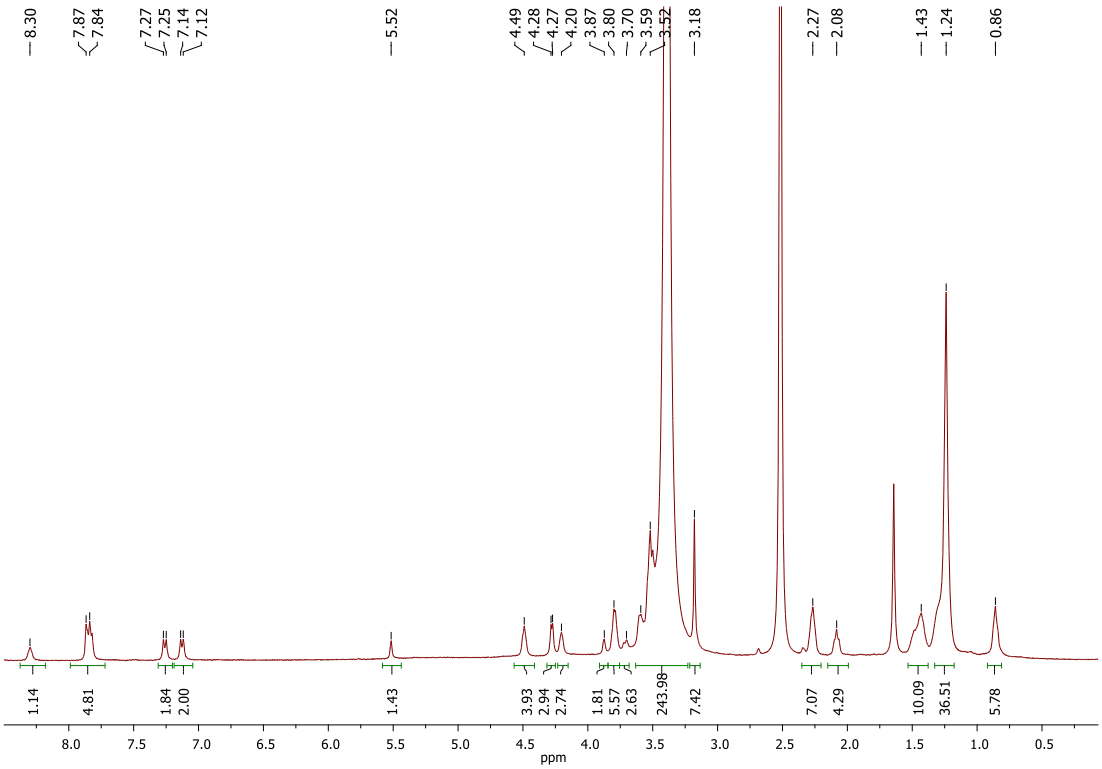

Figure S3. ^{1}H NMR of compound **2** in $DMSOd_6$

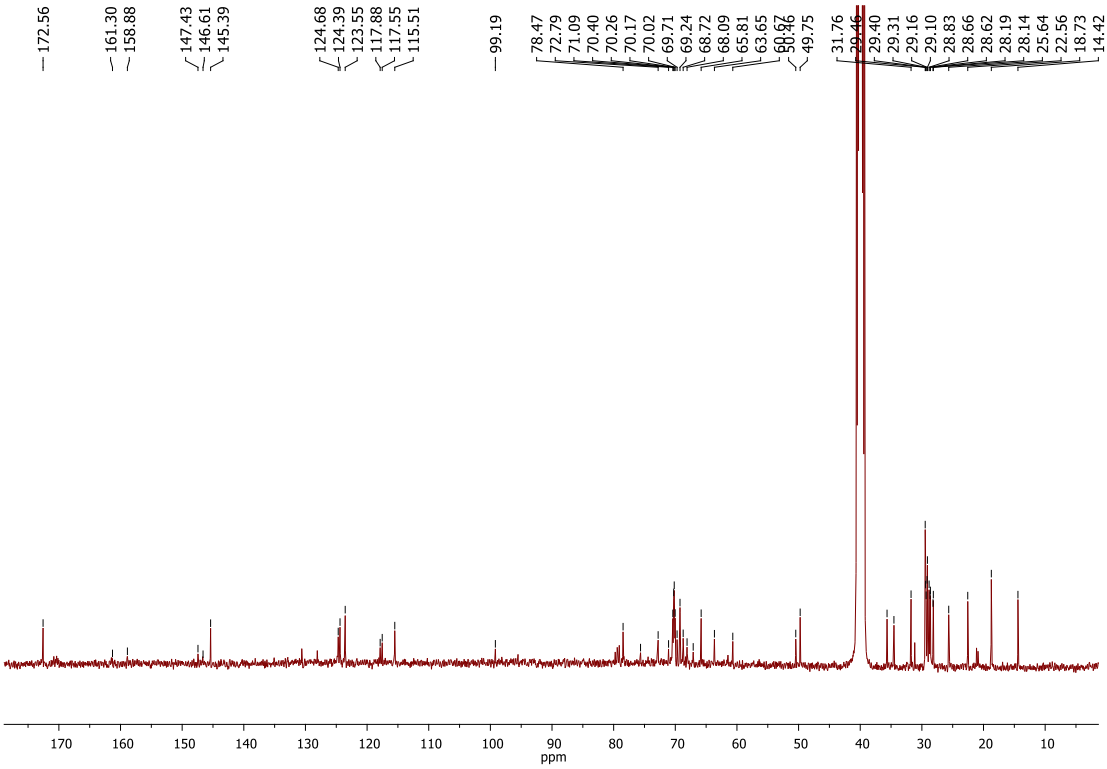

Figure S4. ^{13}C NMR of compound **2** in $DMSOd_6$

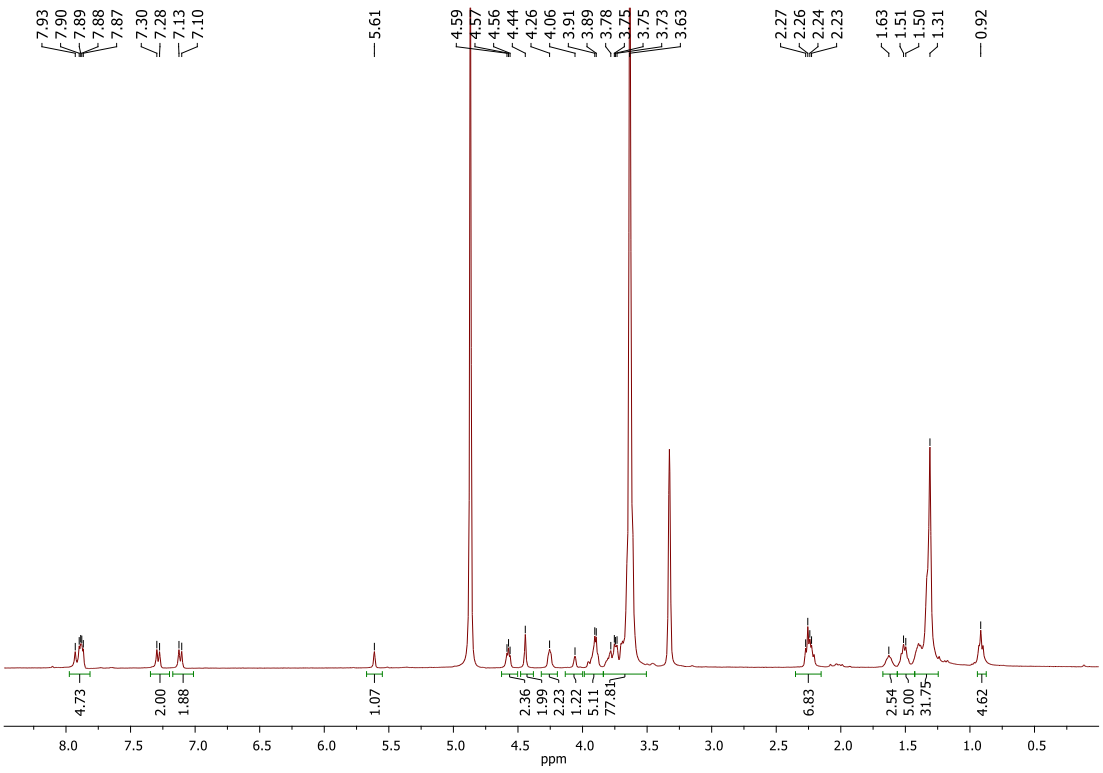

Figure S5. ^{1}H NMR of compound **3** in MeOD

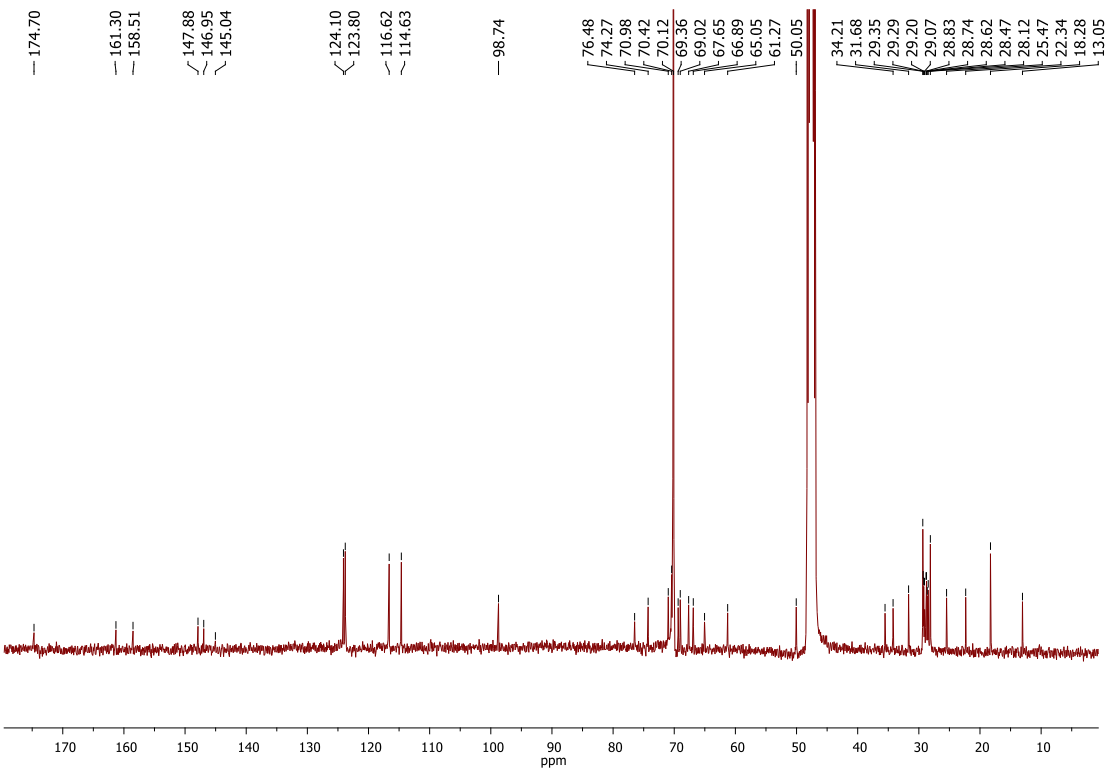

Figure S6. ^{13}C NMR of compound **3** in MeOD

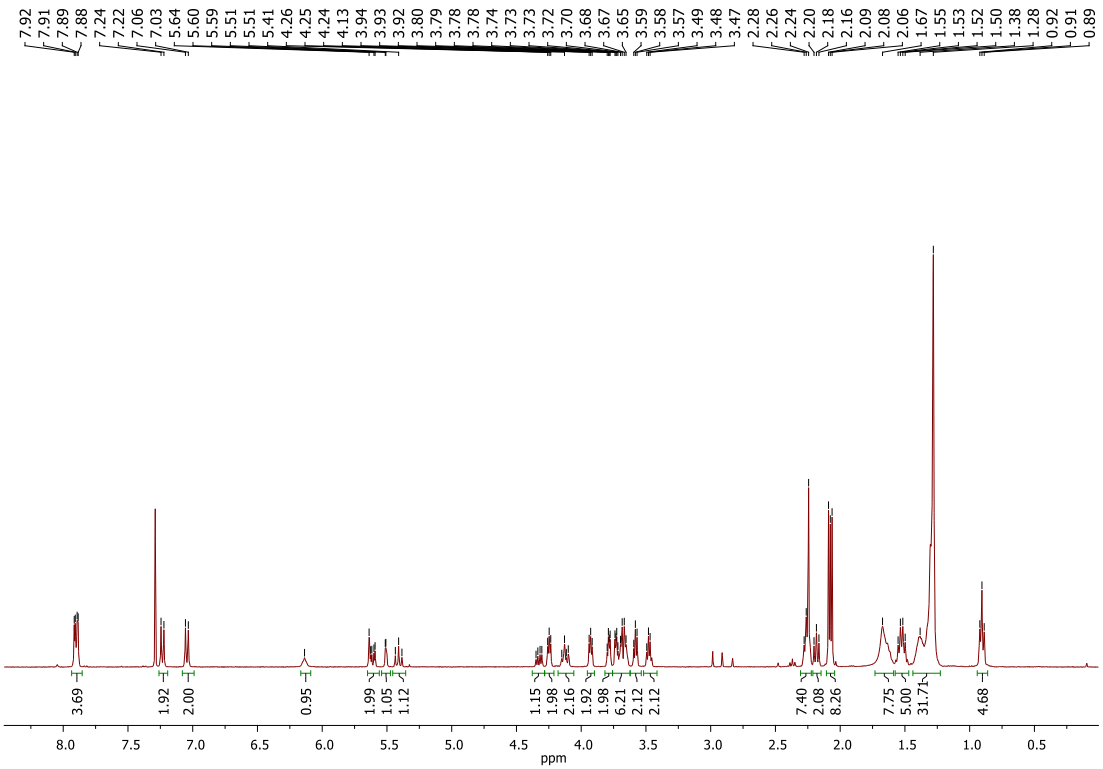

Figure S7. ^{1}H NMR of compound **12** in $CDCl_3$

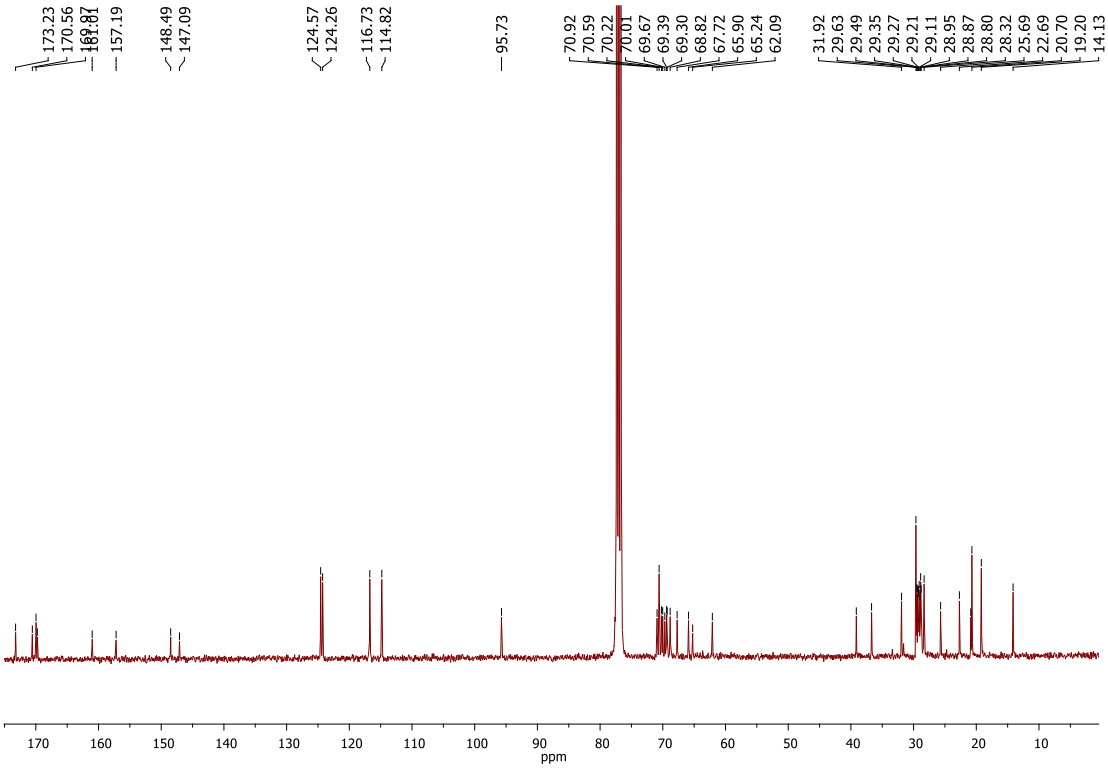

Figure S8. ^{13}C NMR of compound **12** in $CDCl_3$

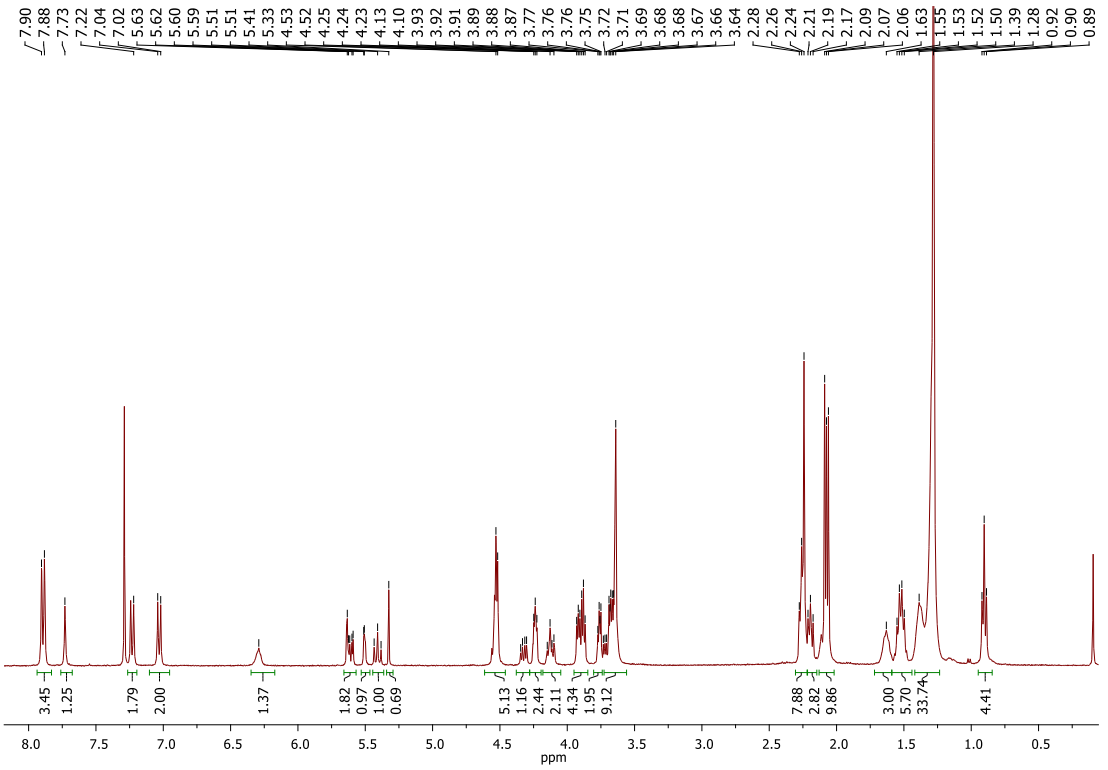

Figure S9. ^{1}H NMR of compound **16** in $CDCl_3$

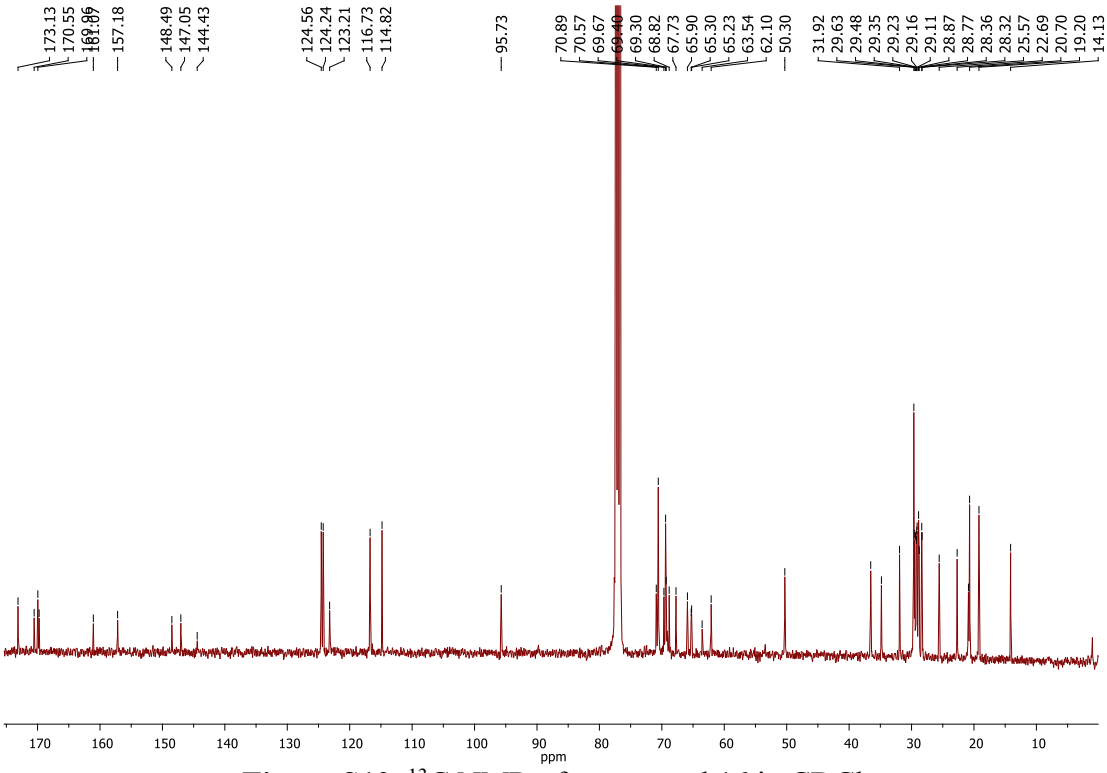

Figure S10. ^{13}C NMR of compound **16** in $CDCl_3$

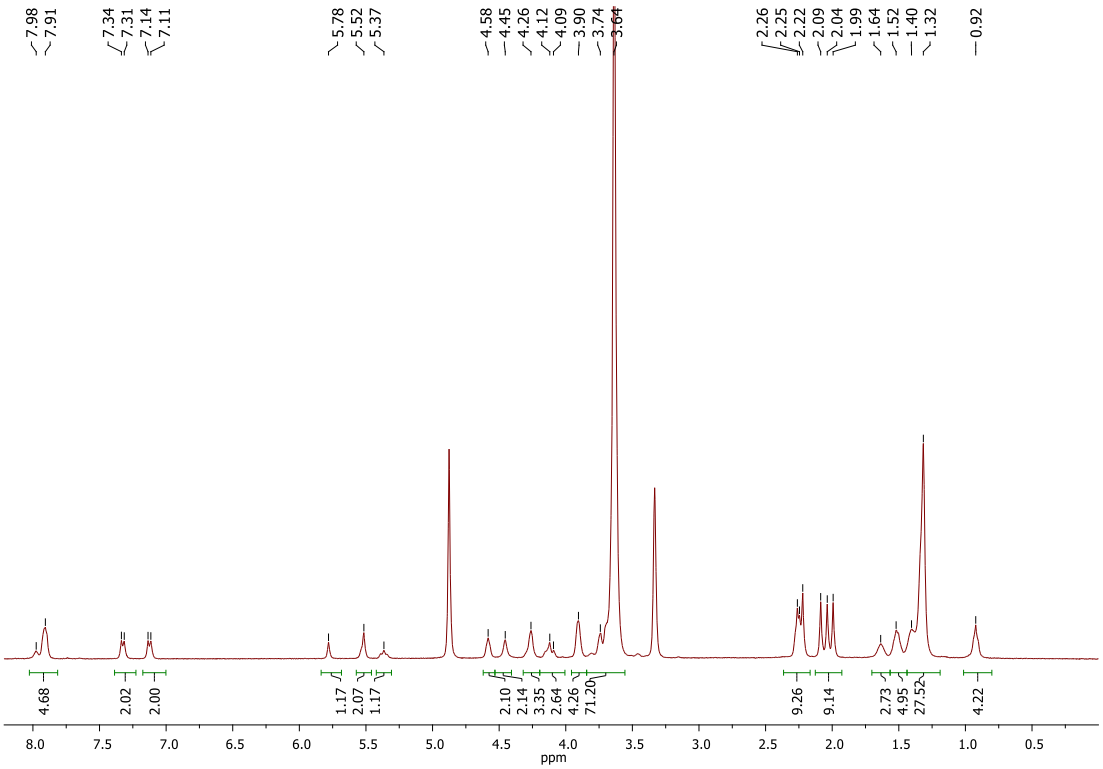

Figure S11. ^{1}H NMR of compound **17** in MeOD

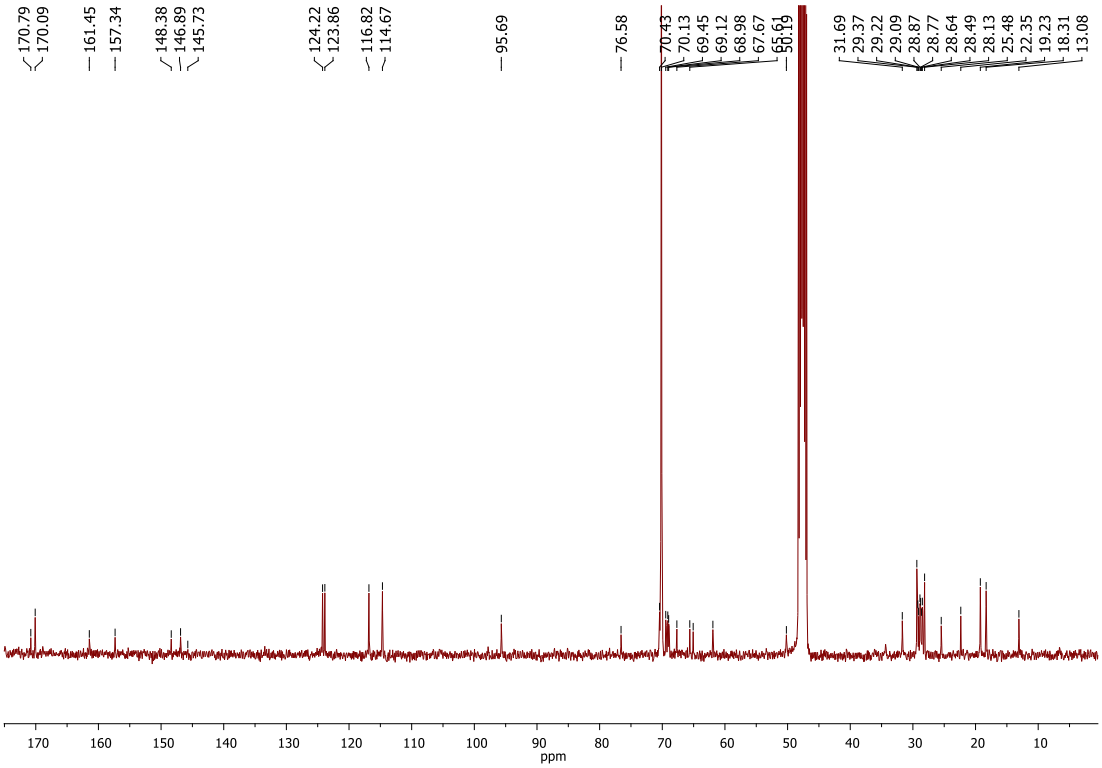

Figure S12. ^{13}C NMR of compound **17** in MeOD

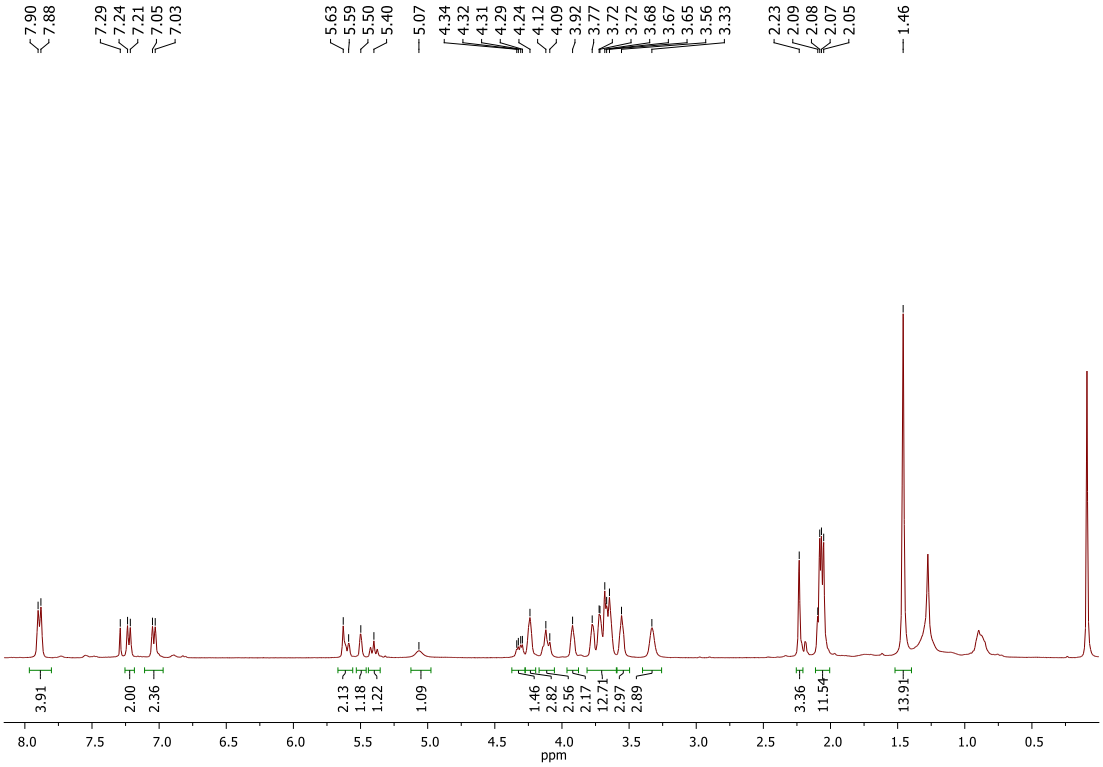

Figure S13. ^{1}H NMR of compound **10** in $CDCl_3$

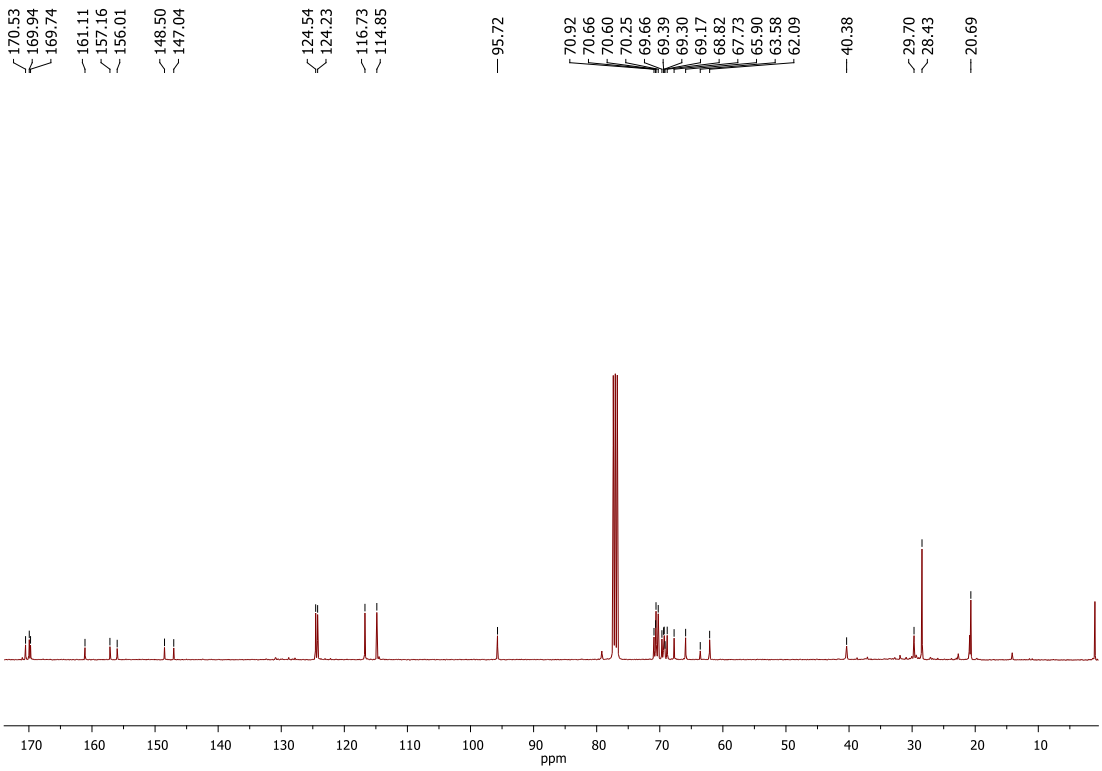

Figure S14. ^{13}C NMR of compound **10** in $CDCl_3$

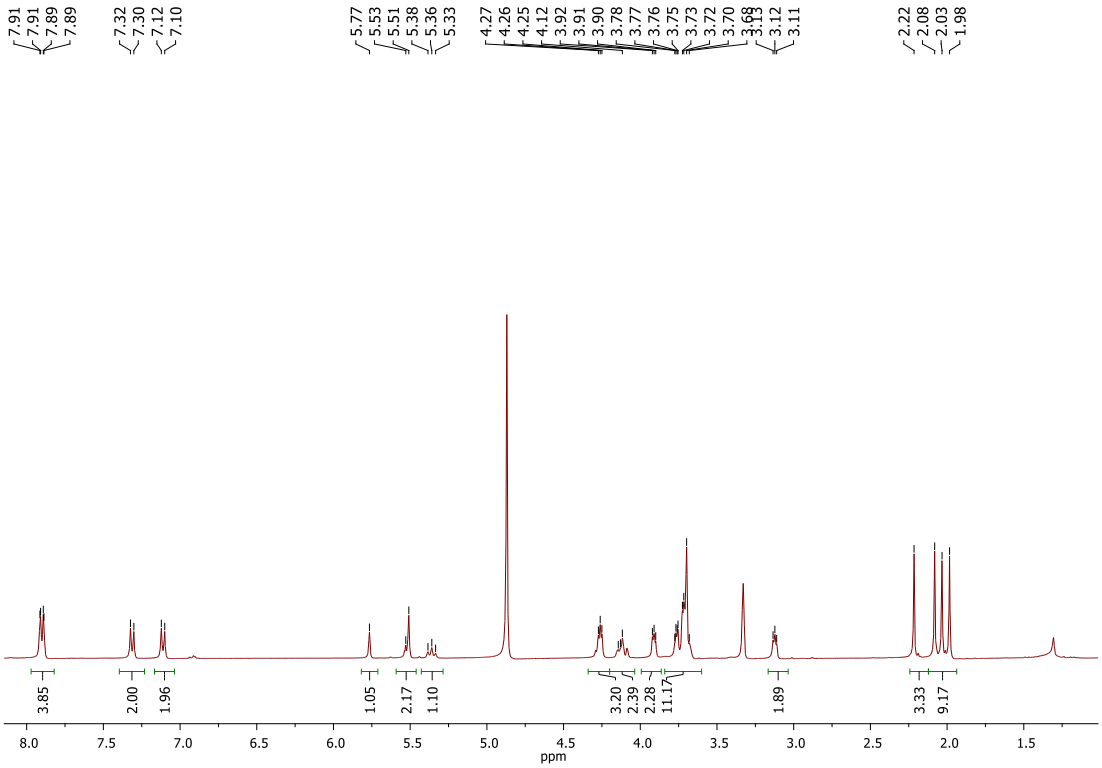

Figure S15. ^{1}H NMR of compound **11** in MeOD

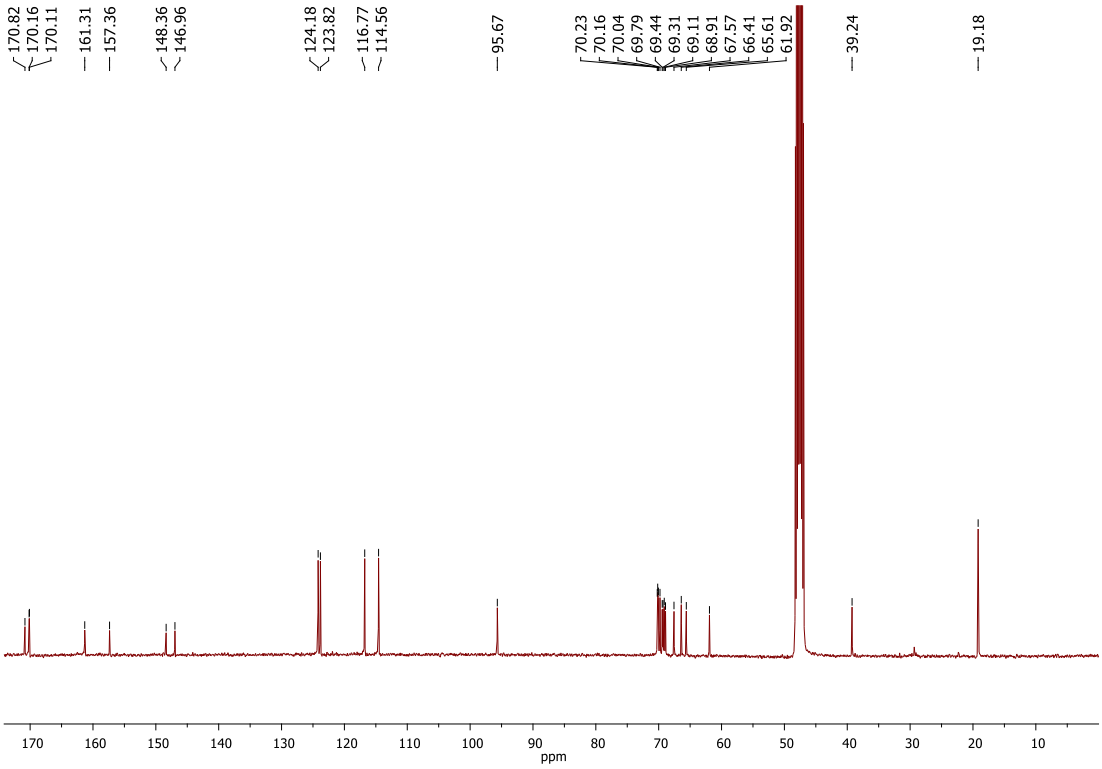

Figure S16. ^{1}H NMR of compound **11** in MeOD

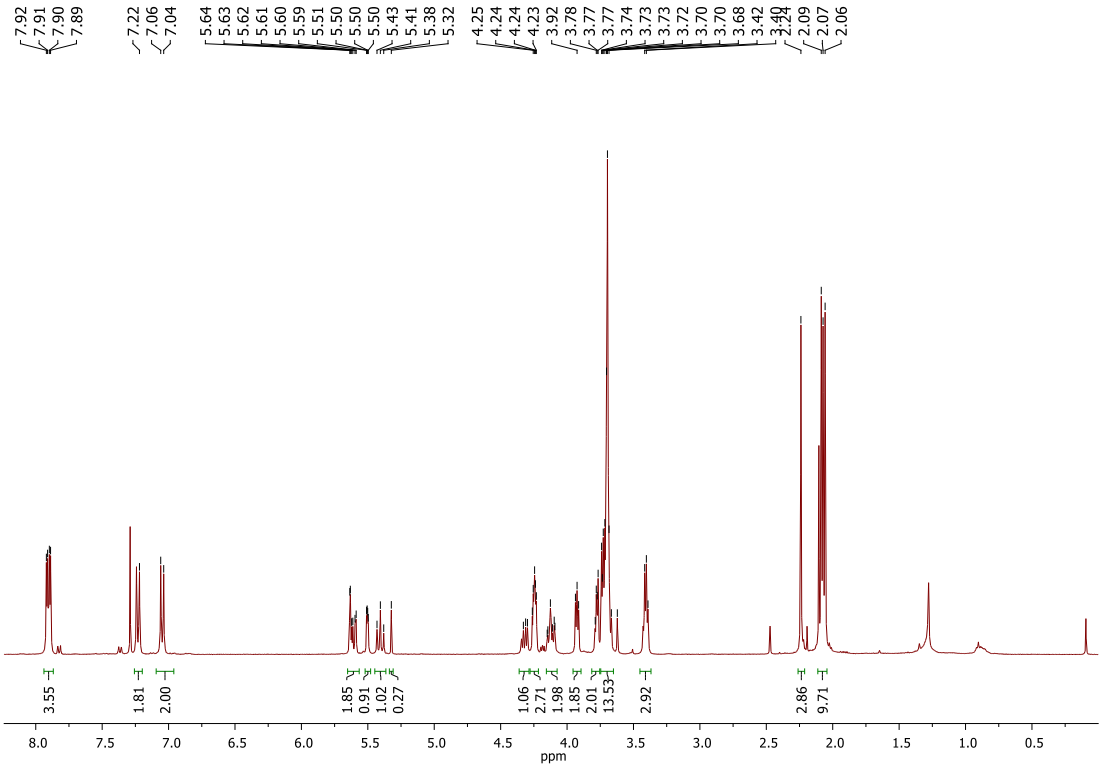

Figure S17. ^{1}H NMR of compound **13** in $CDCl_3$

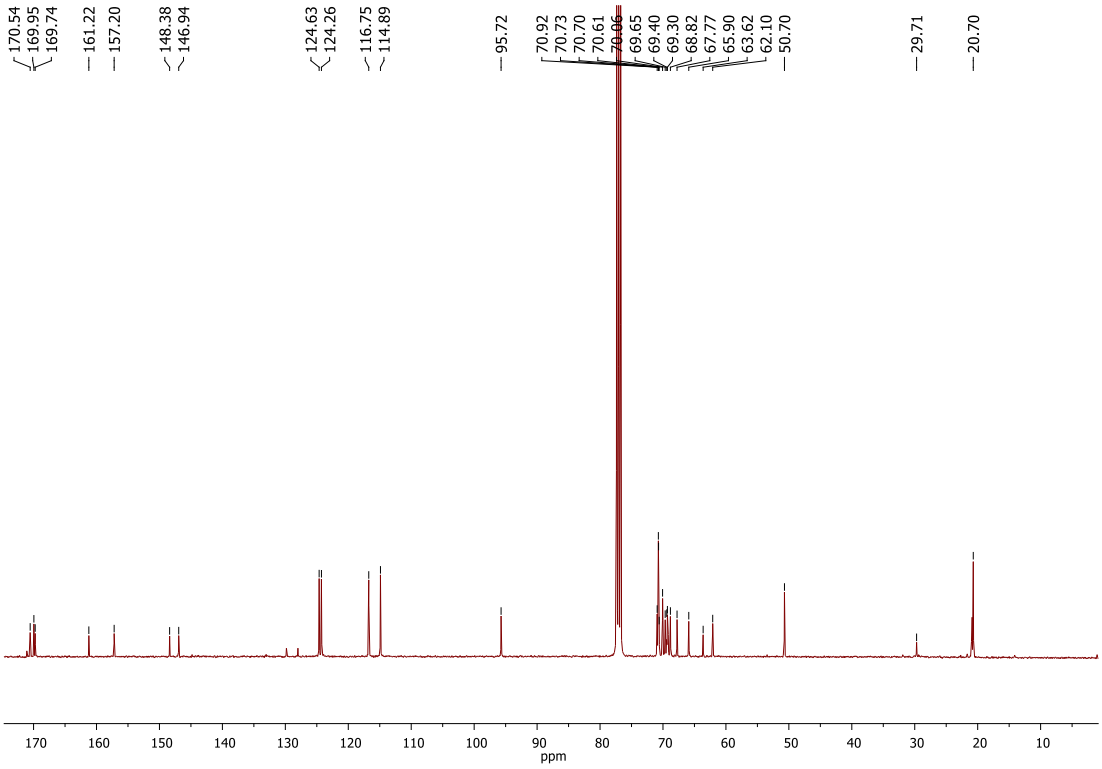

Figure S18. ^{13}C NMR of compound **13** in $CDCl_3$

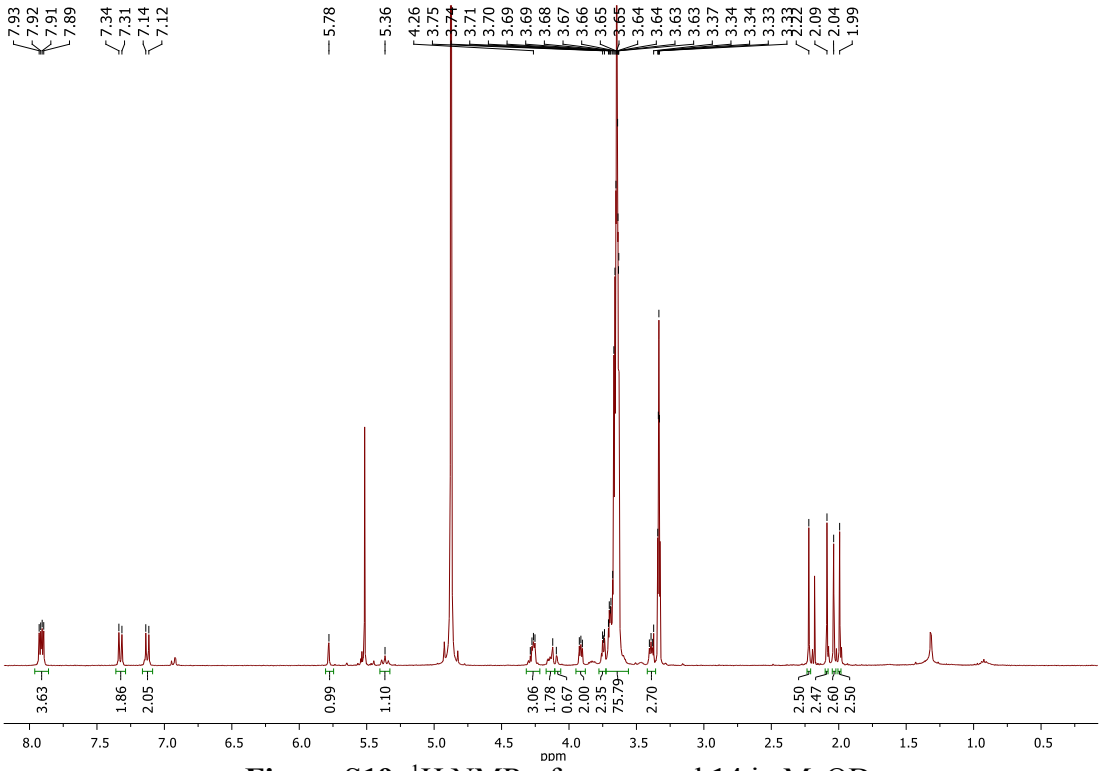

Figure S19. ^{1}H NMR of compound **14** in MeOD

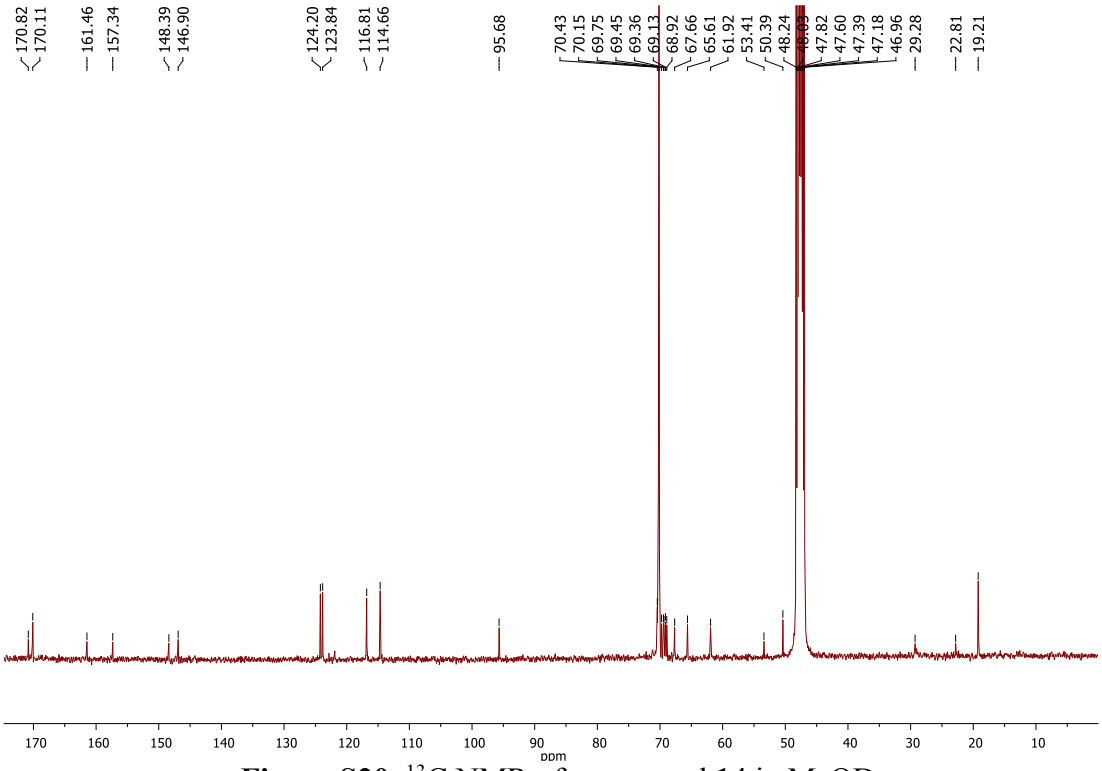

Figure S20. ^{13}C NMR of compound **14** in MeOD

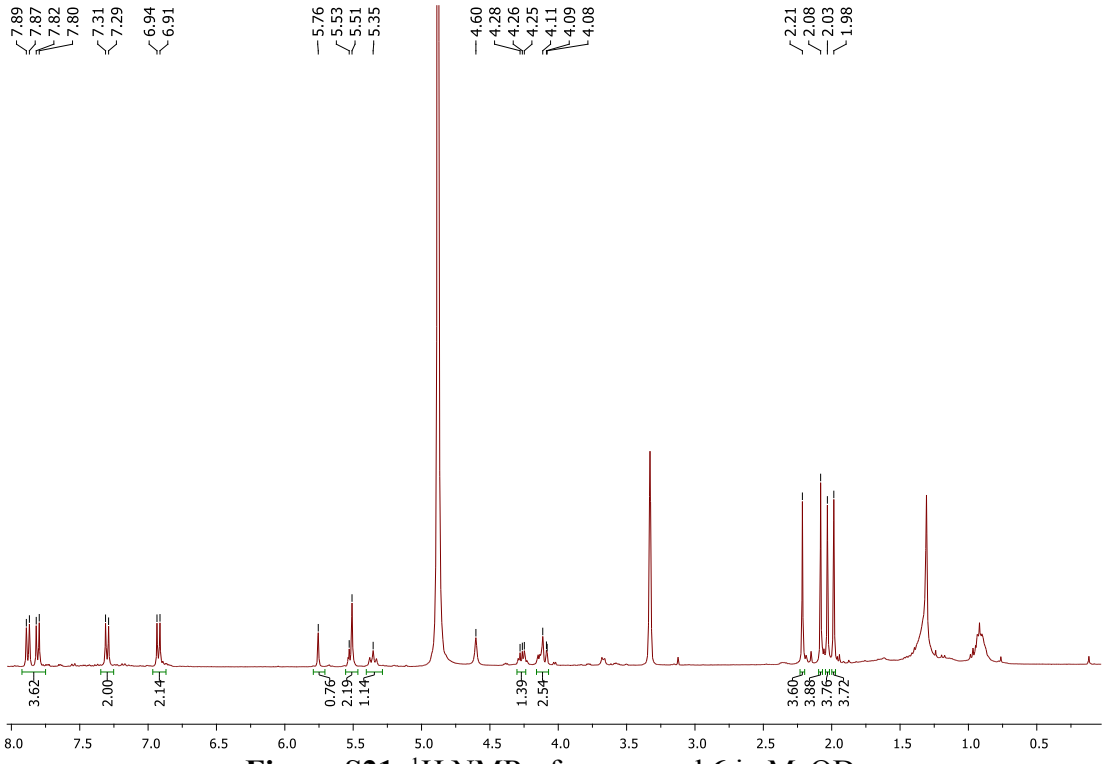

Figure S21. ^{1}H NMR of compound **6** in MeOD

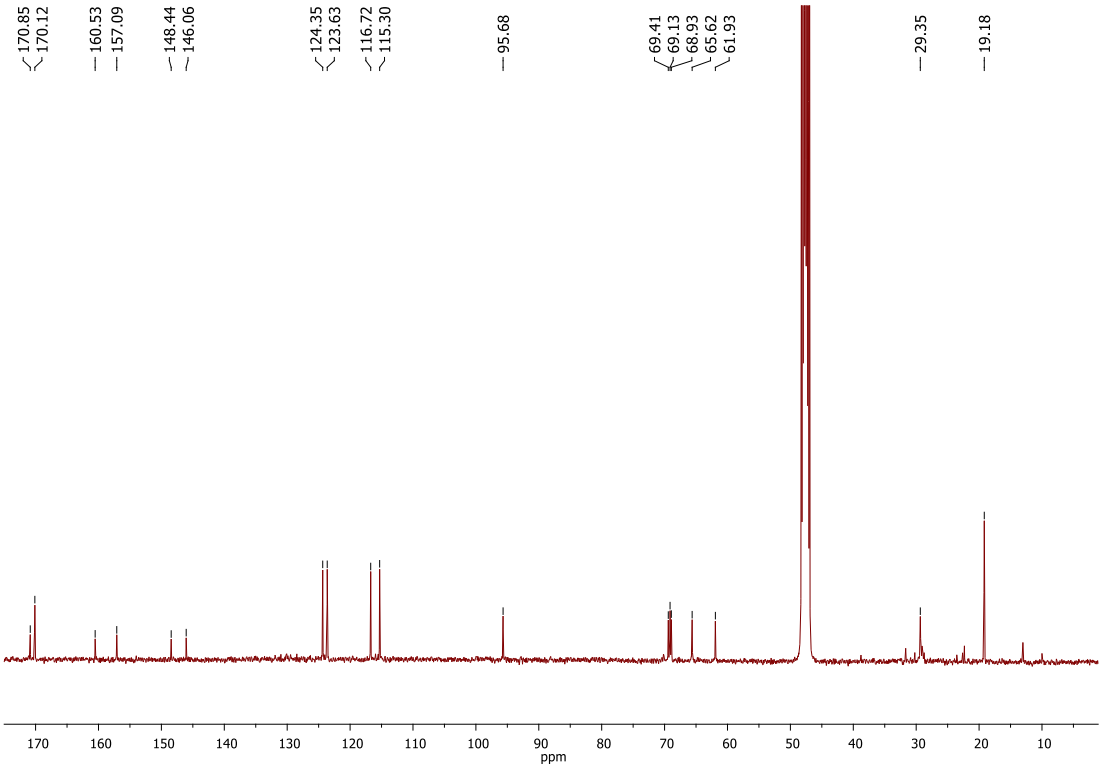

Figure S22. ^{13}C NMR of compound **6** in MeOD

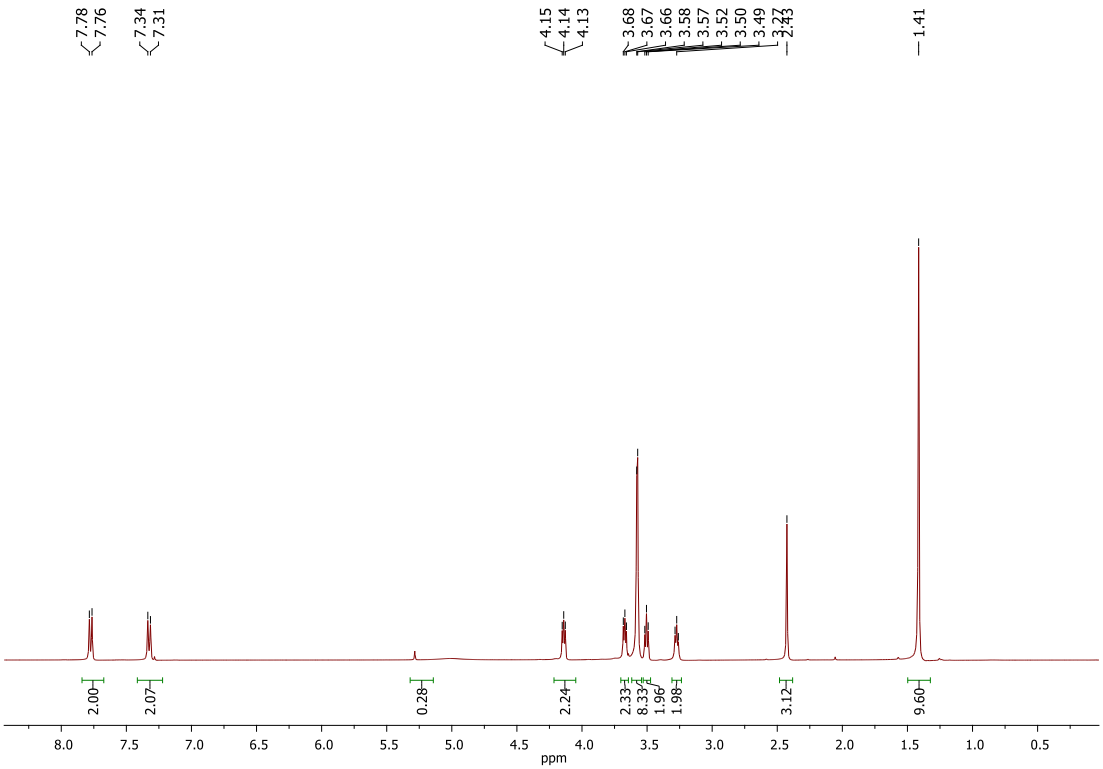

Figure S23. ^{1}H NMR of compound **7** in $CDCl_3$

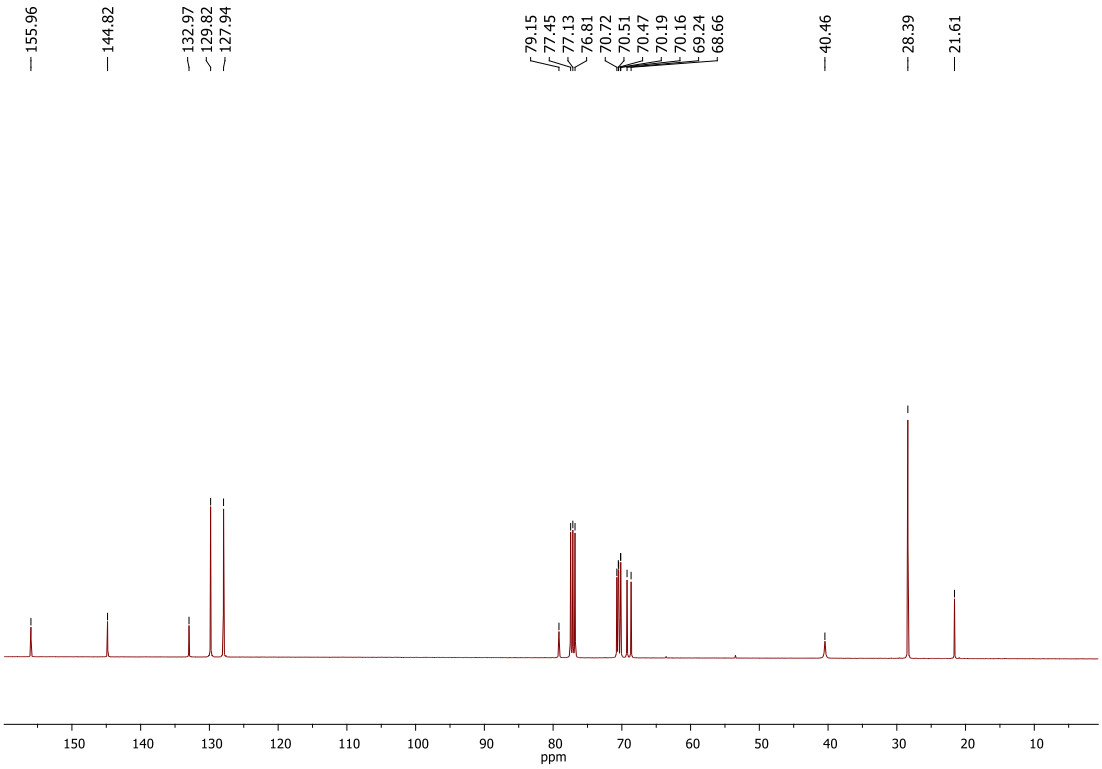

Figure S24. ^{13}C NMR of compound **7** in $CDCl_3$

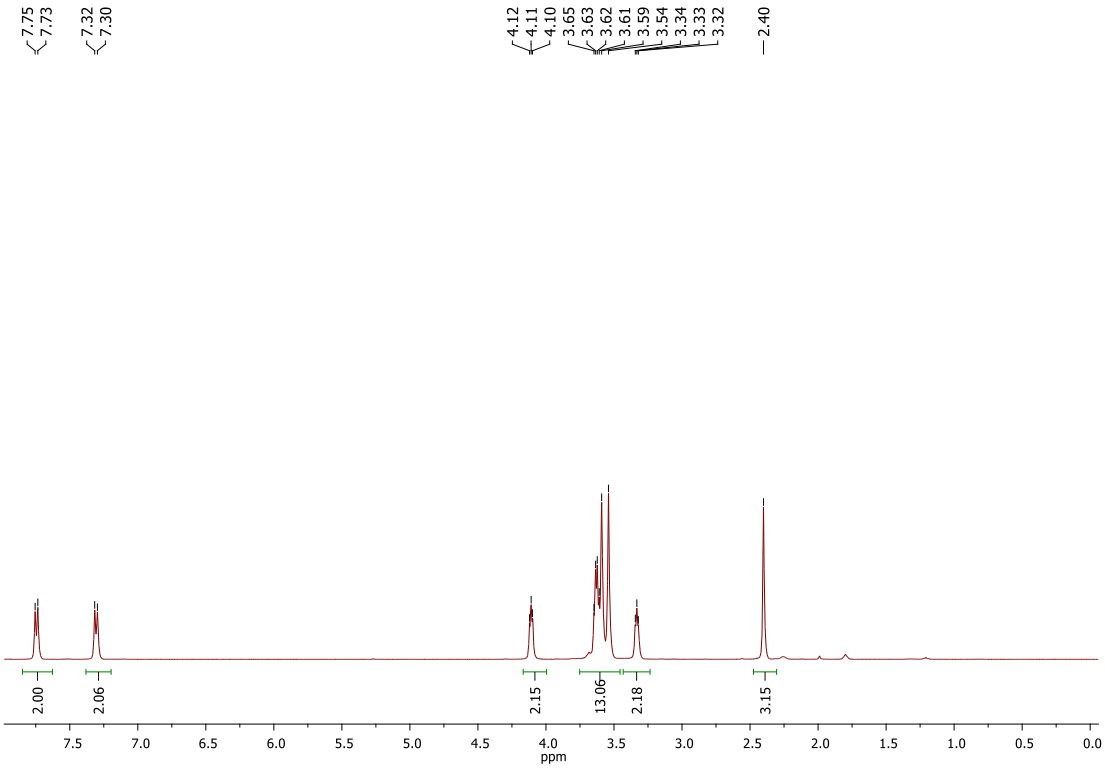

Figure S25. ^{1}H NMR of compound **8** in $CDCl_3$

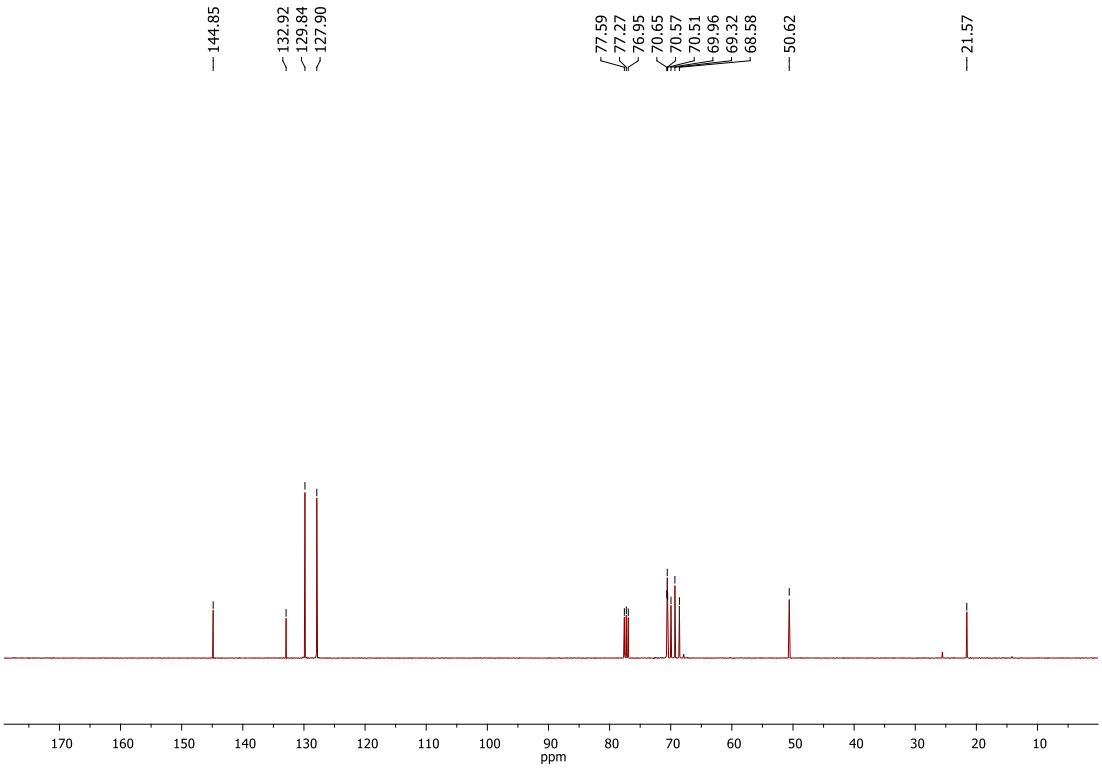

Figure S26. ^{13}C NMR of compound **8** in $CDCl_3$

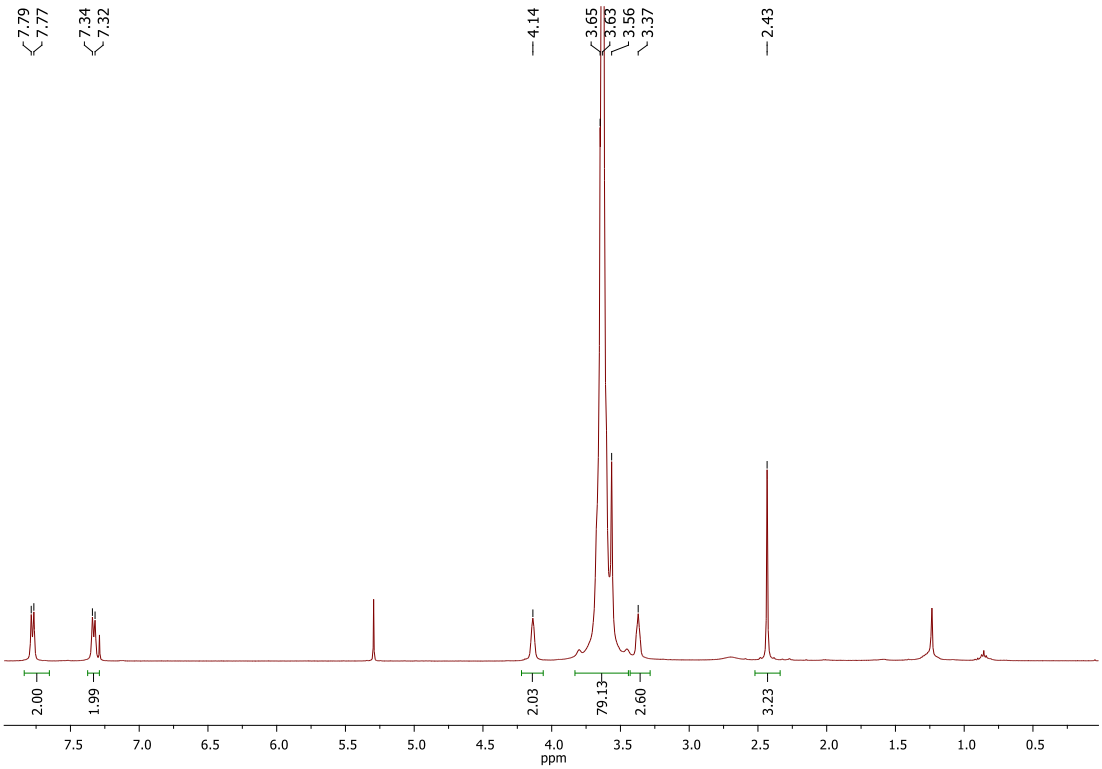

Figure S27. ^{1}H NMR of compound **9** in $CDCl_3$

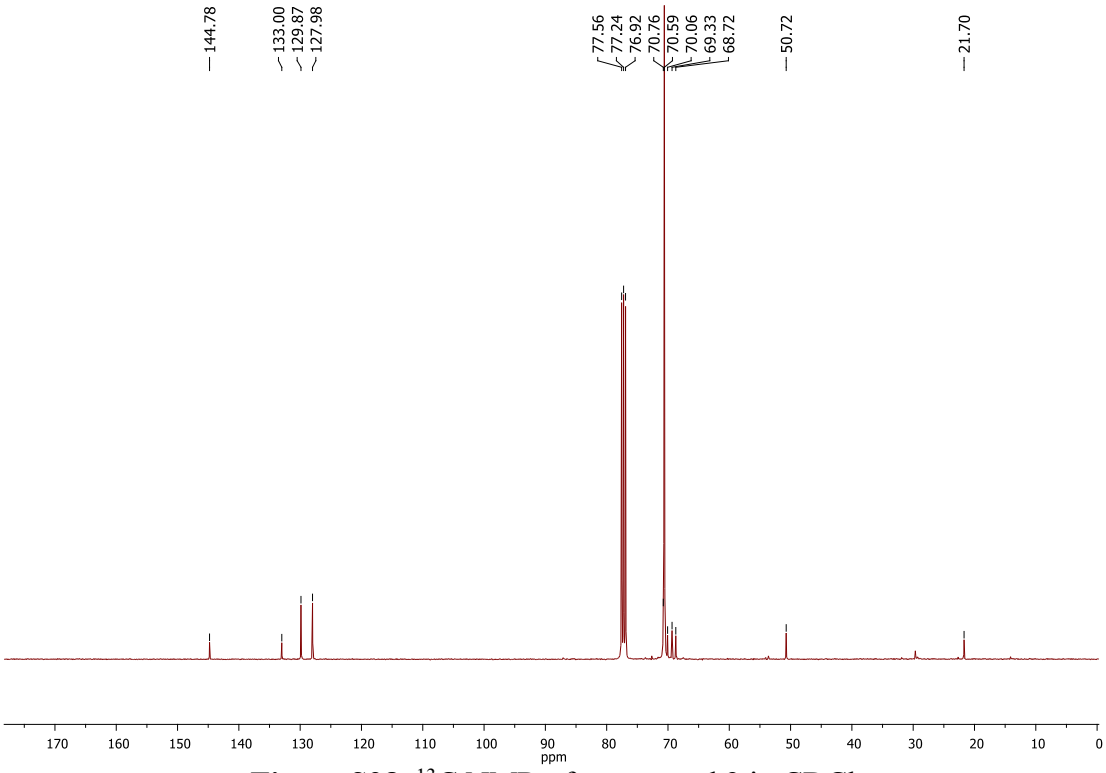

Figure S28. ^{13}C NMR of compound **9** in $CDCl_3$

3. HRMS SPECTRA

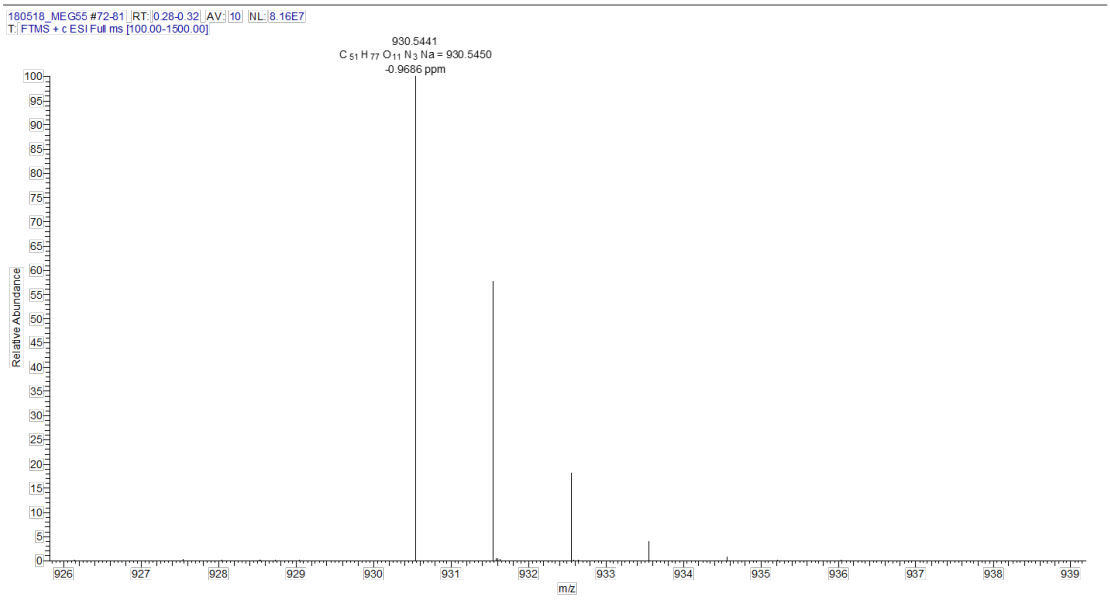

Figure S29. HRMS of compound **1**

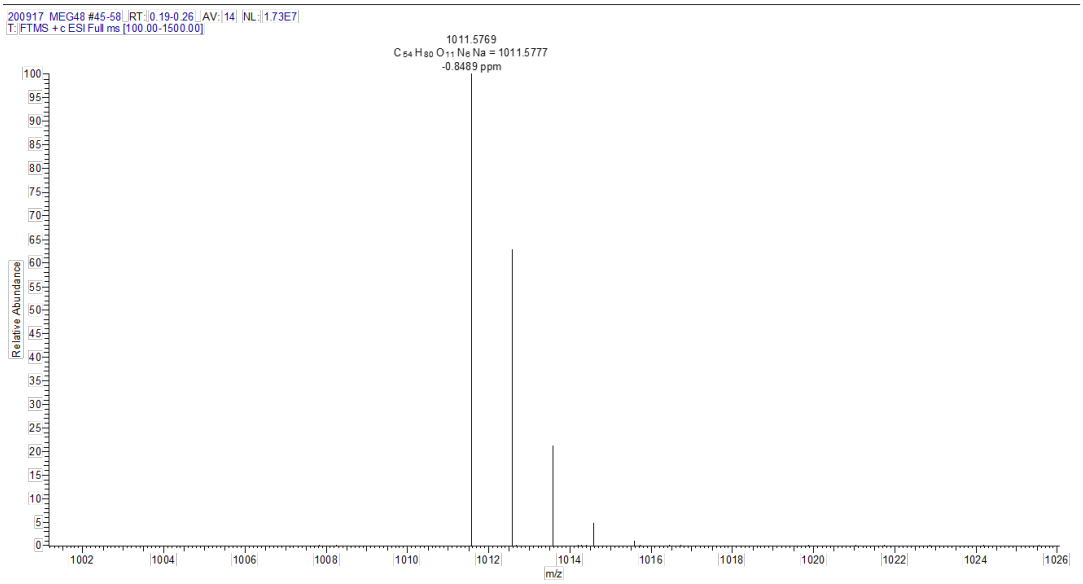

Figure S30. HRMS of compound **2**

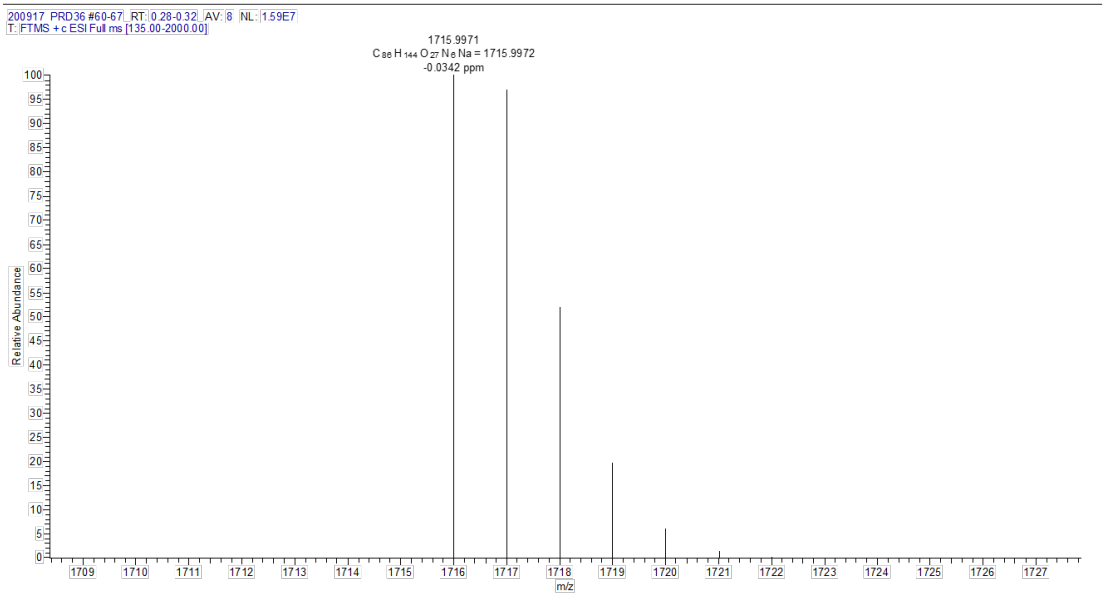

Figure S31. HRMS of compound **3**

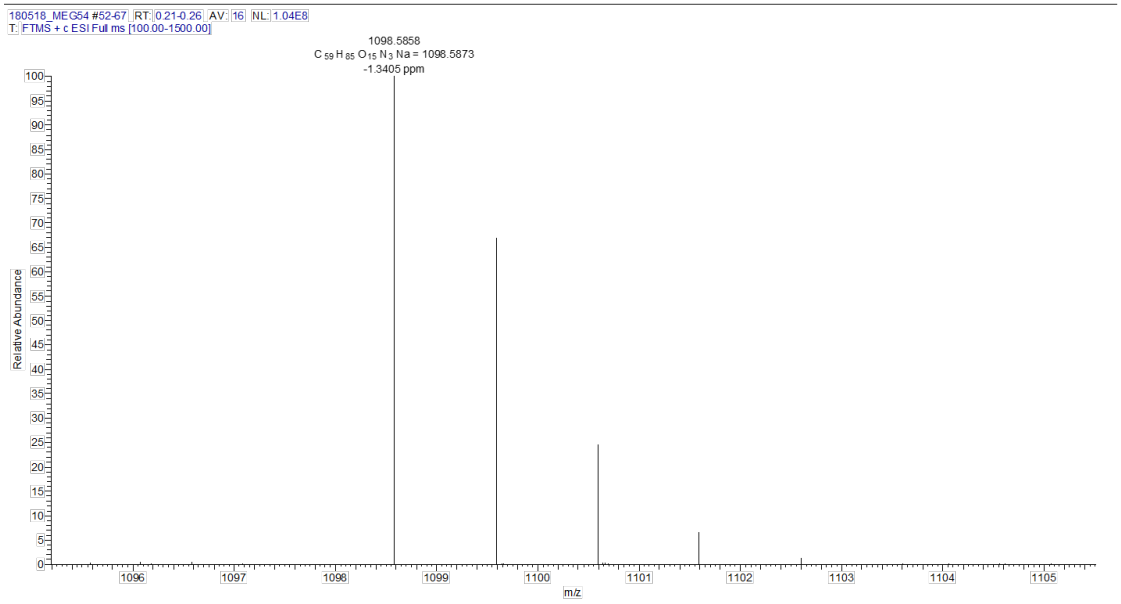

Figure S32. HRMS of compound **12**

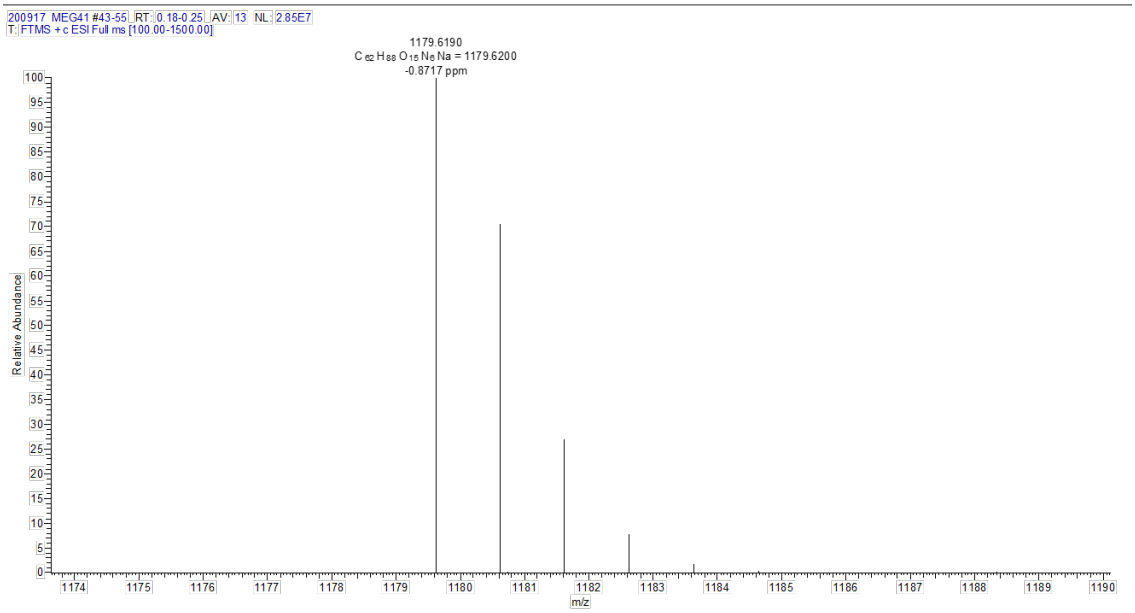

Figure S33. HRMS of compound **16**

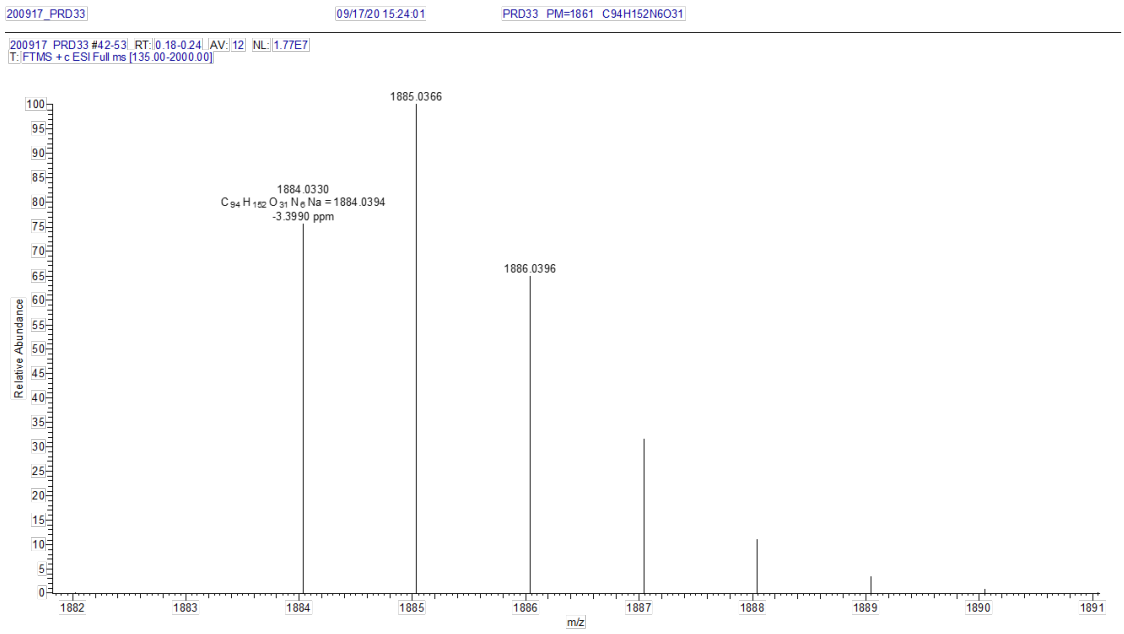

Figure S34. HRMS of compound **17**

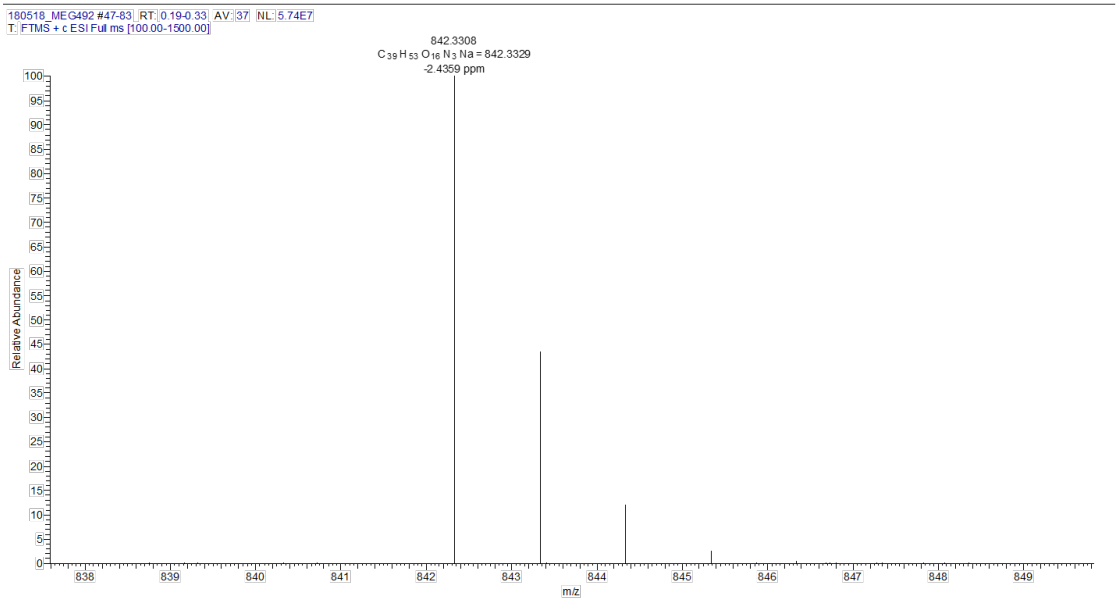

Figure S35. HRMS of compound **10**

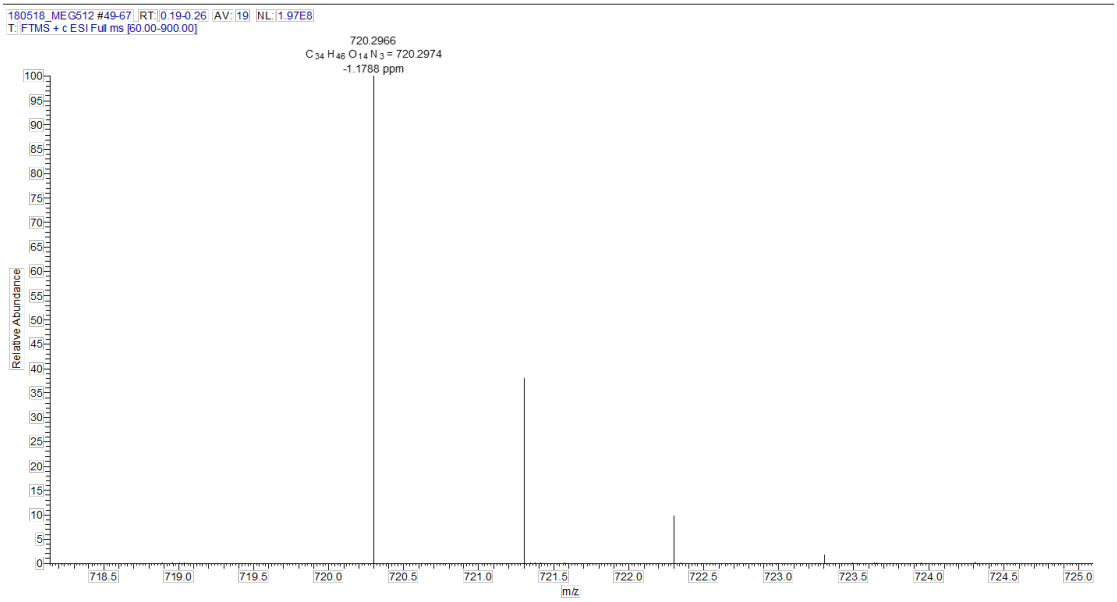

Figure S36. HRMS of compound **11**

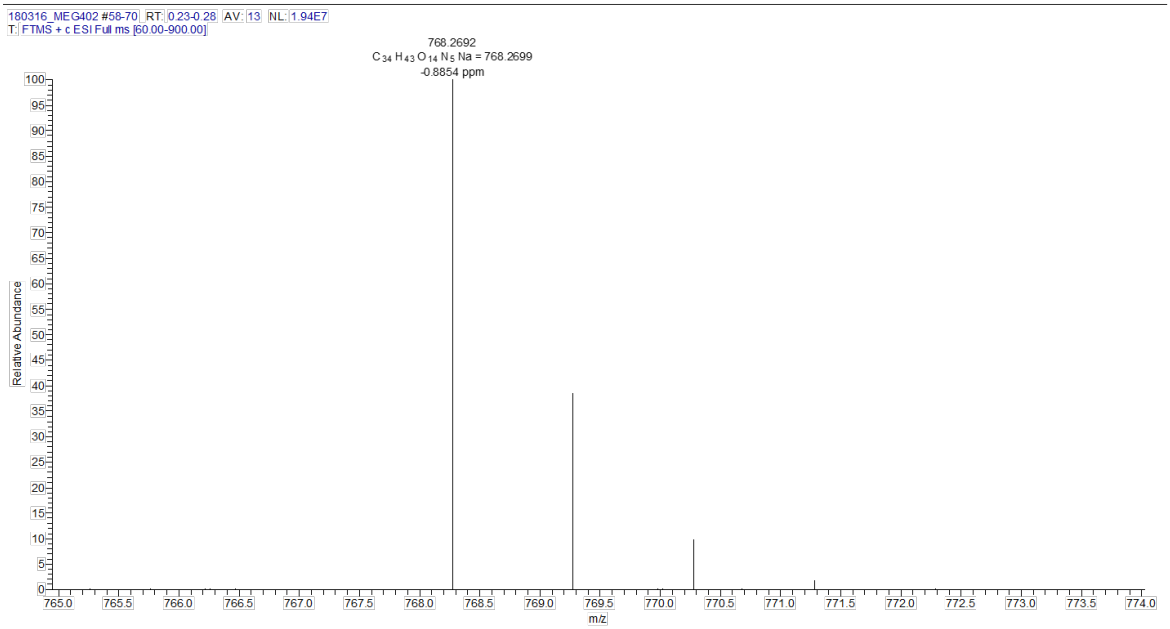

Figure S37. HRMS of compound **13**

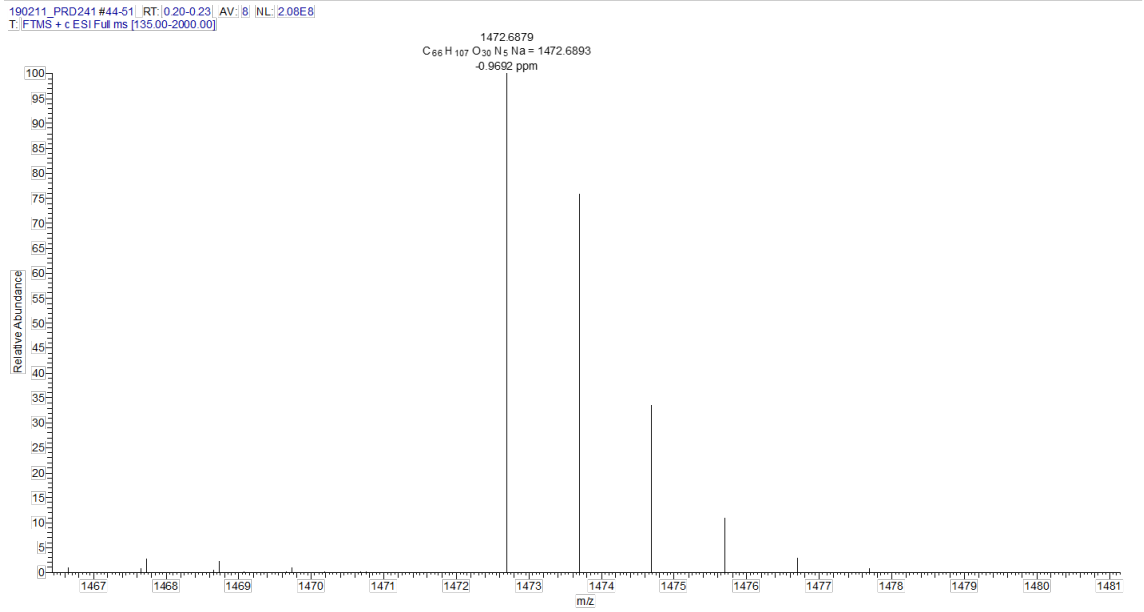

Figure S38. HRMS of compound **14**

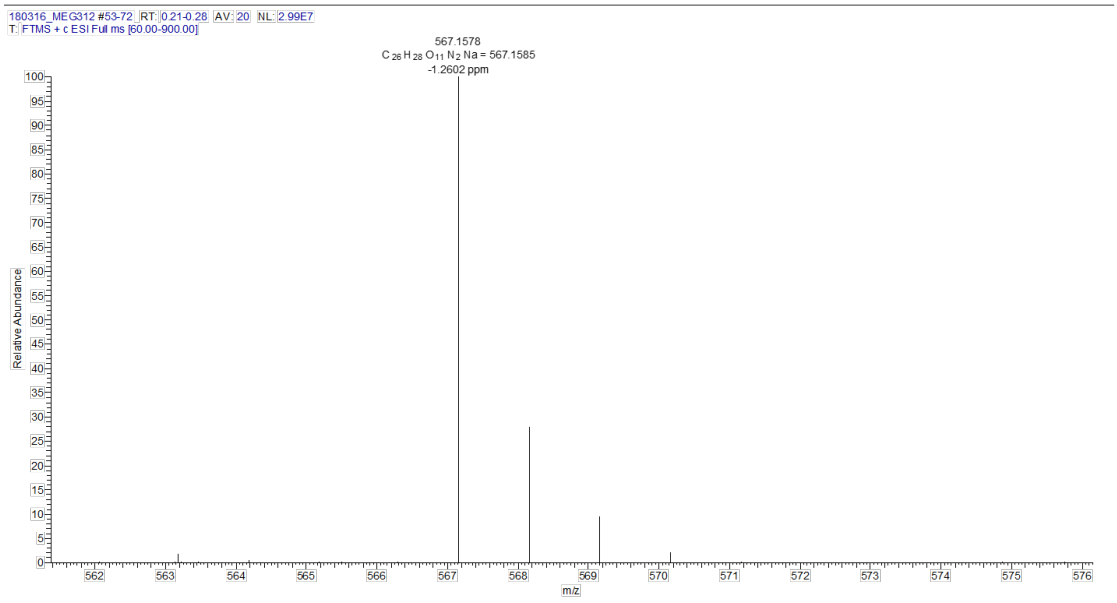

Figure S39. HRMS of compound **6**

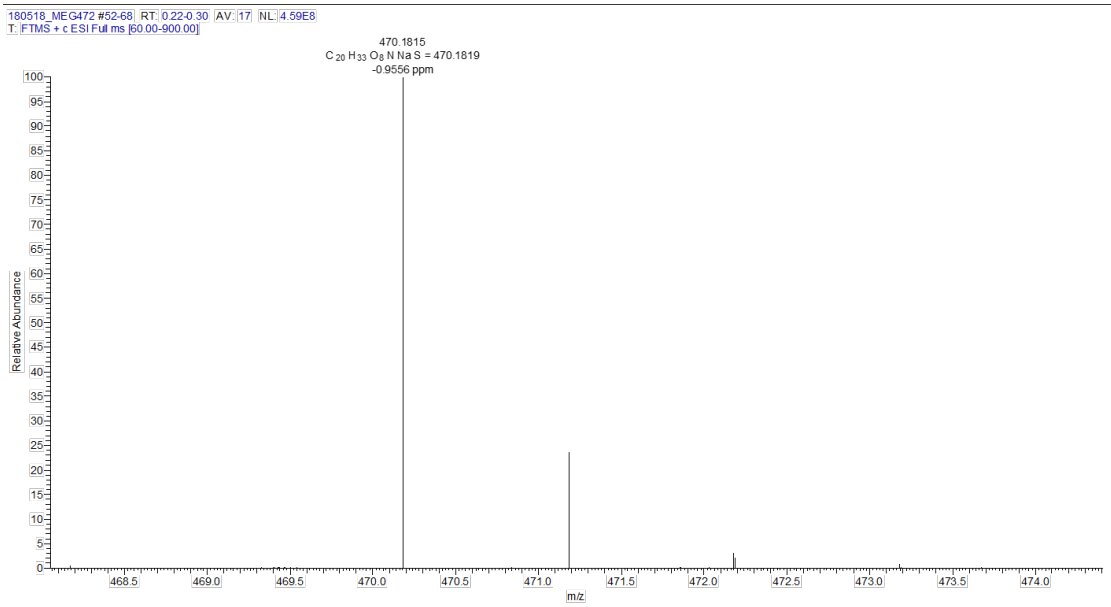

Figure S40. HRMS of compound **7**

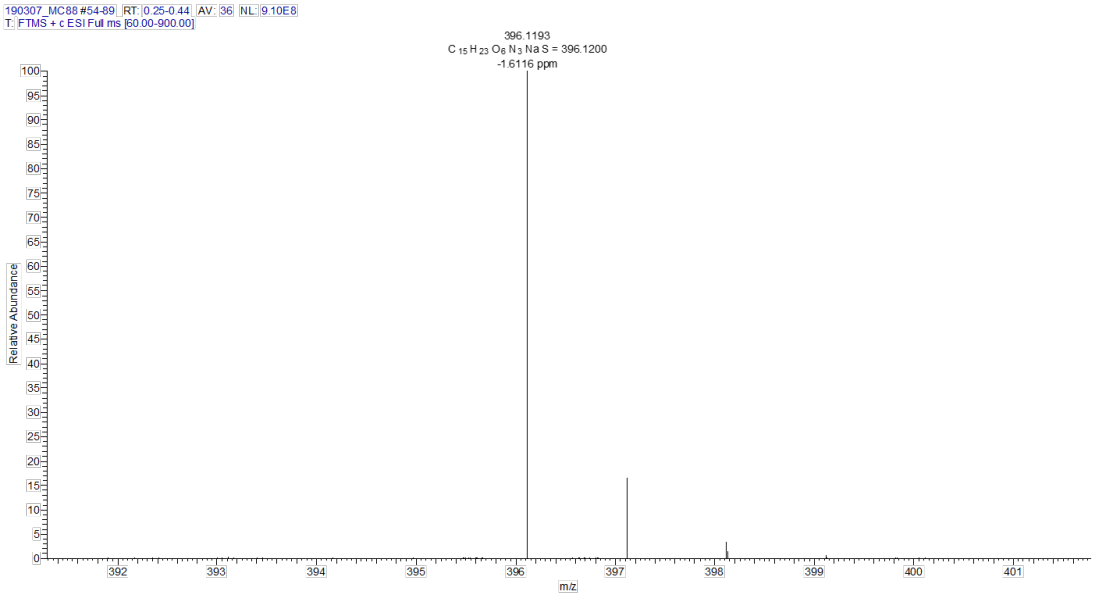

Figure S41. HRMS of compound **8**

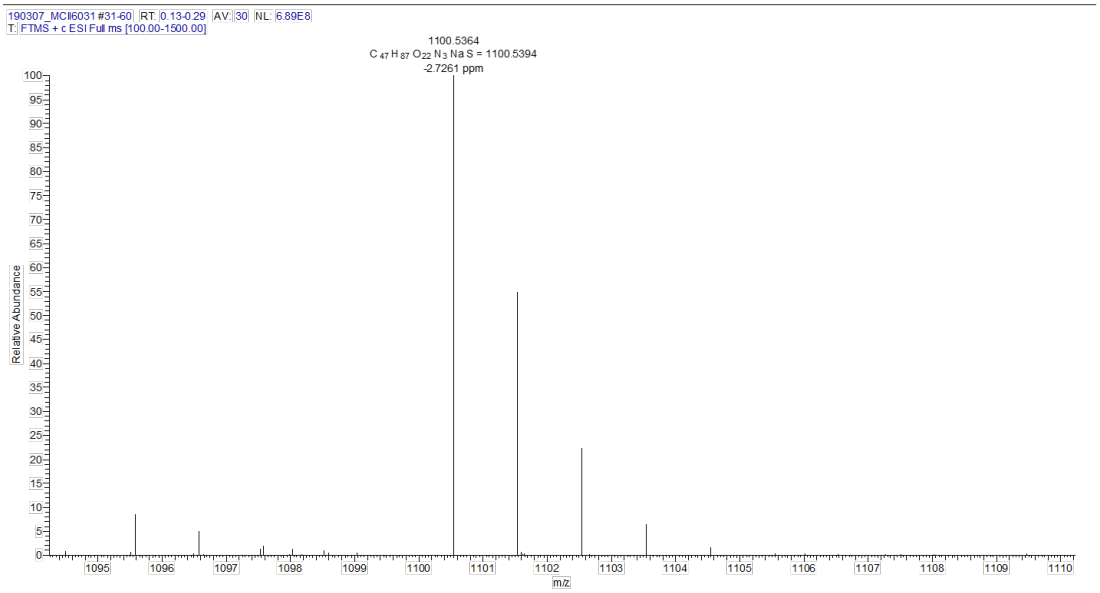

Figure S42:.HRMS of compound **9**

4. TEM AND SEM IMAGES

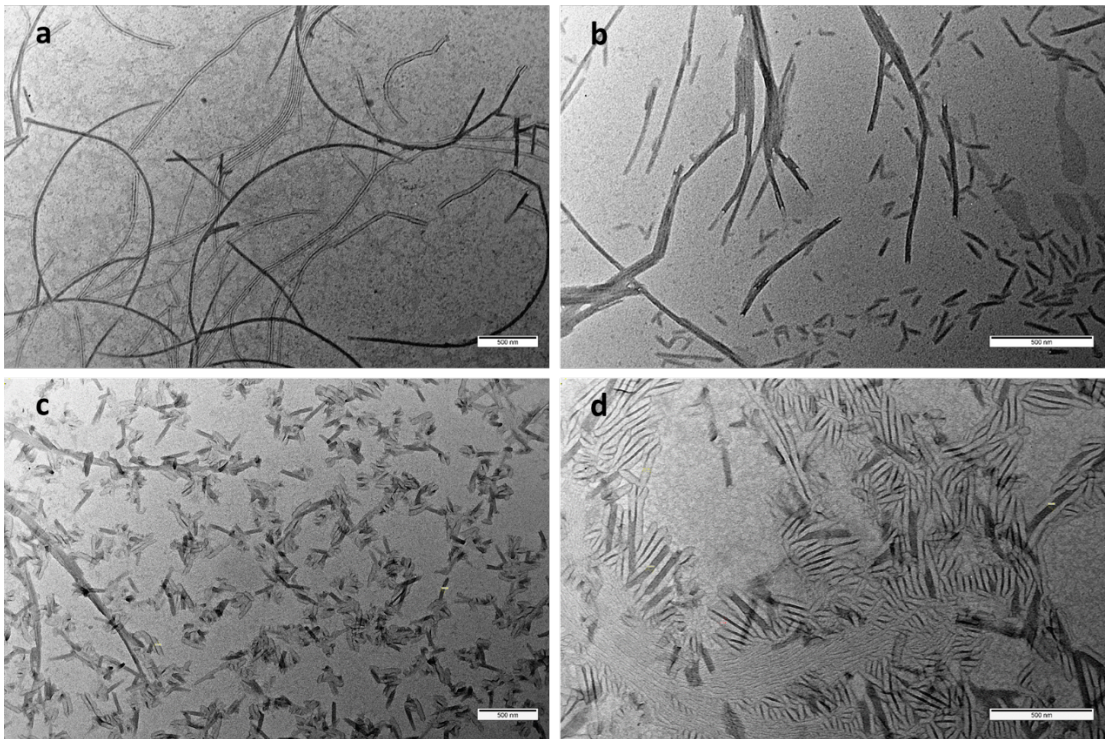

Figure S43. TEM images of Lipid Nanotubes (LNTs) formed by supramolecular self-organization of *trans* **1** in 50% aqueous ethanol (a and b). TEM images of LNTs formed by supramolecular self-organization of *cis* **1** in 50% aqueous ethanol (c and d).

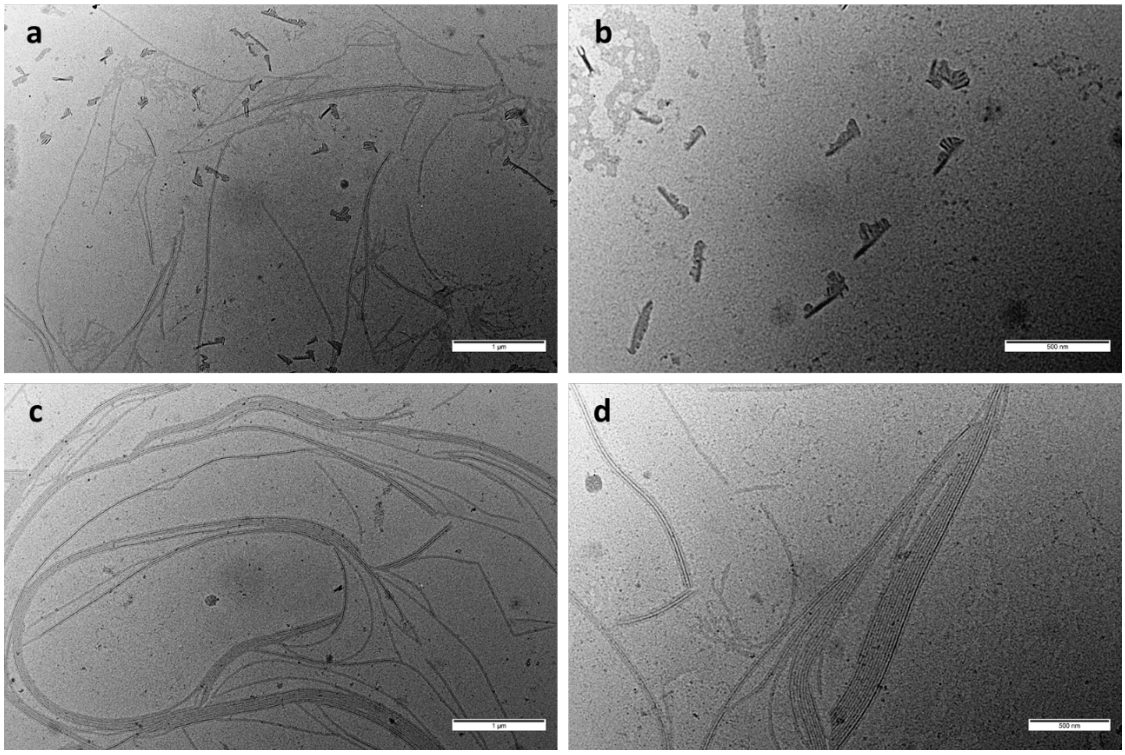

Figure S44. TEM study of supramolecular self-organization of *trans* **1** in water (a-d).

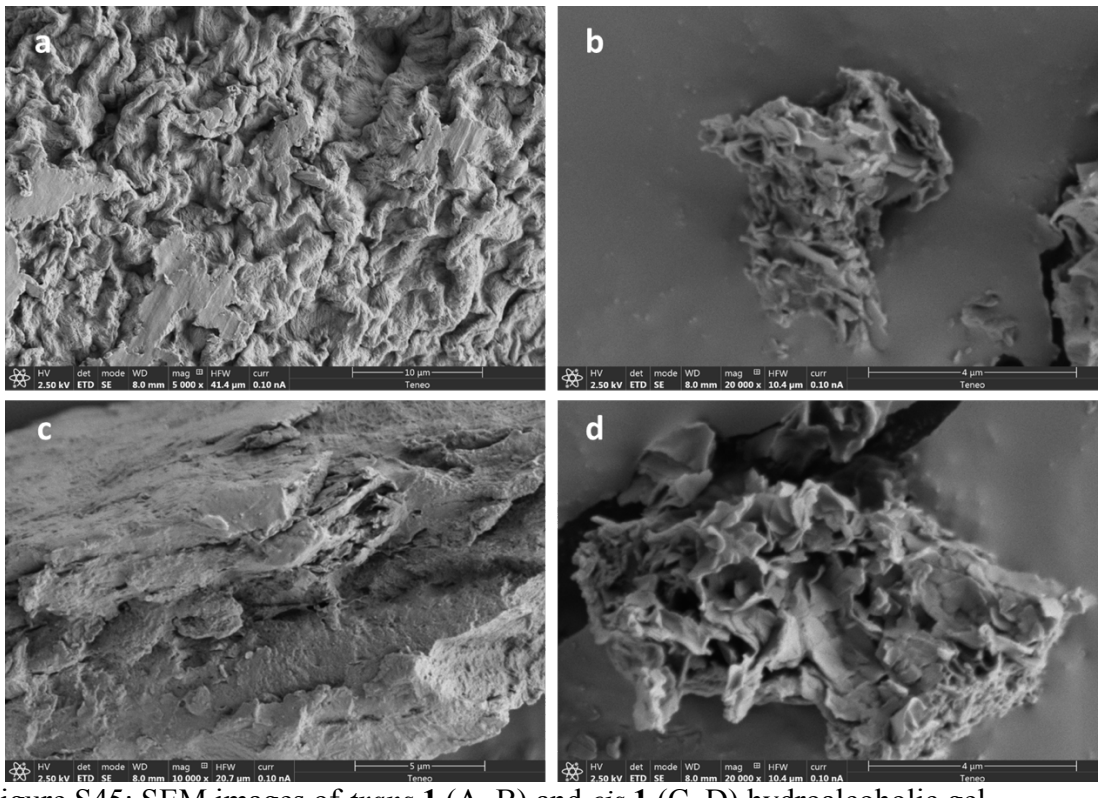

Figure S45: SEM images of *trans* **1** (A, B) and *cis* **1** (C, D) hydroalcoholic gel.

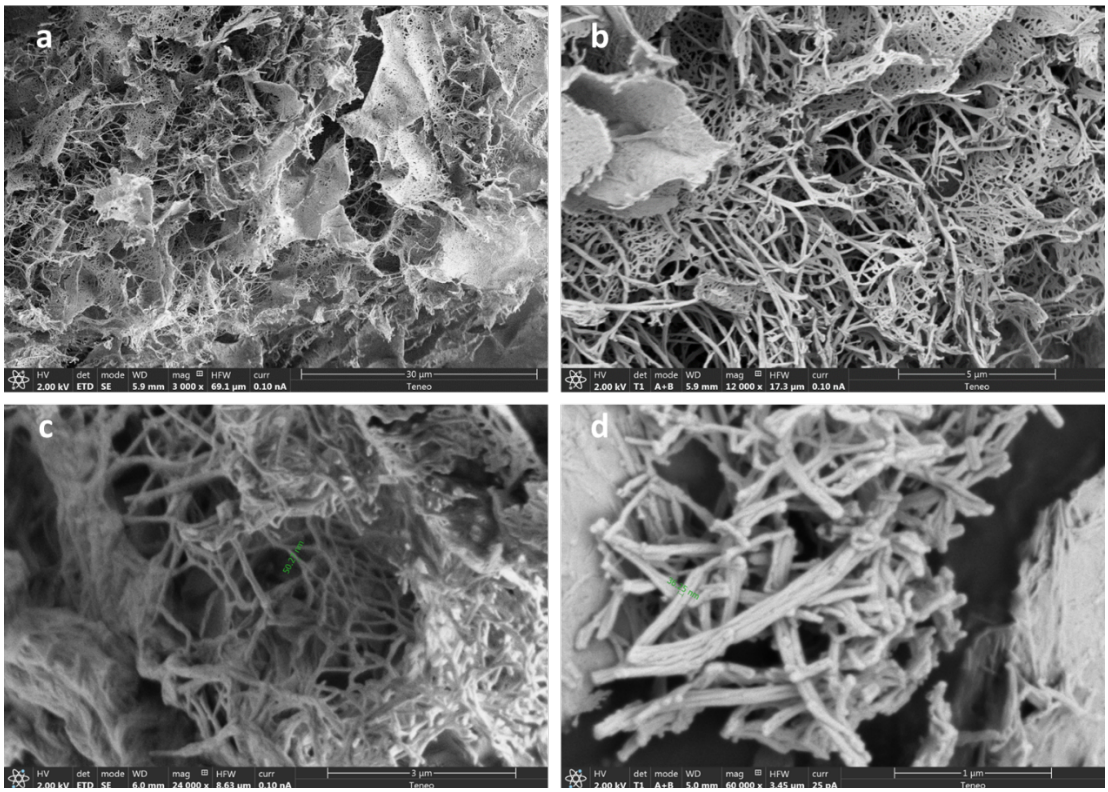

Figure S46. SEM images of *trans* **1** xerogel (a-d).

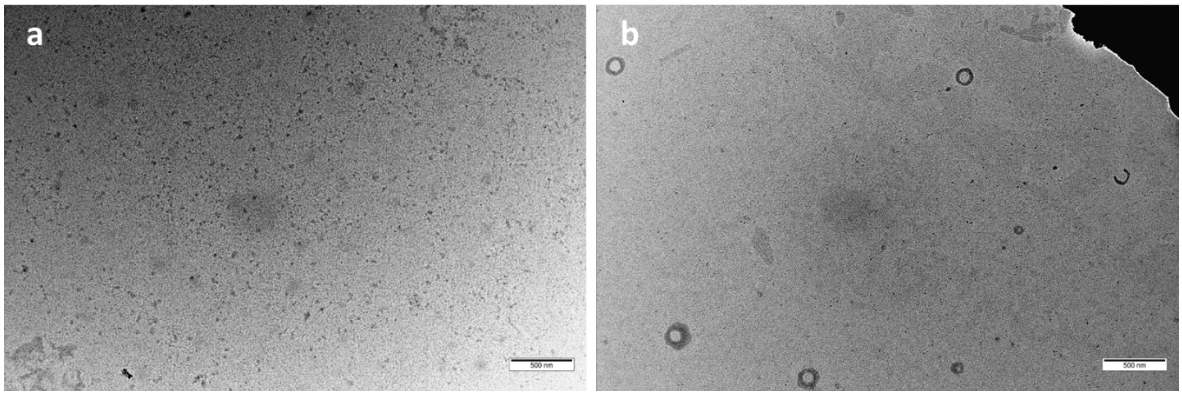

Figure S47. TEM images of spherical micelles (a) and liposomes (b) formed by supramolecular self-organization of **3** in water.

5. ISOMERIZATION STUDIES

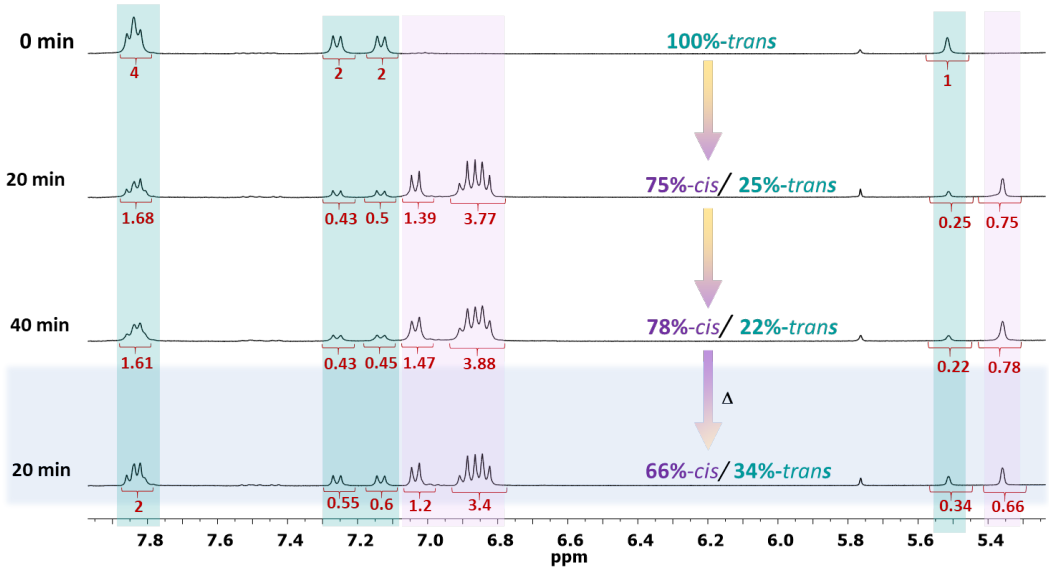

Figure S48. [1]HNMR photoisomerization *trans-cis* studies of neoglycolipid **1** in DMSO-d_6. The blue box indicates the *cis-trans* isomerization in dark conditions.

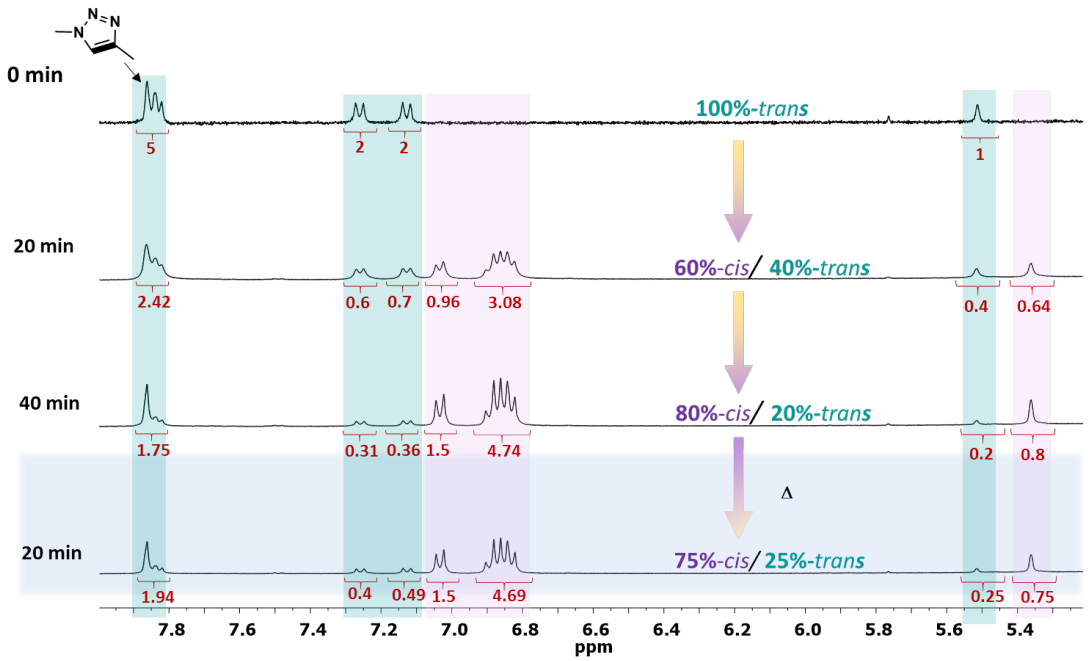

Figure S49. [1]HNMR photoisomerization *trans-cis* studies of compound **2** in DMSO-d_6. The blue box indicates *cis-trans* isomerization in dark conditions.

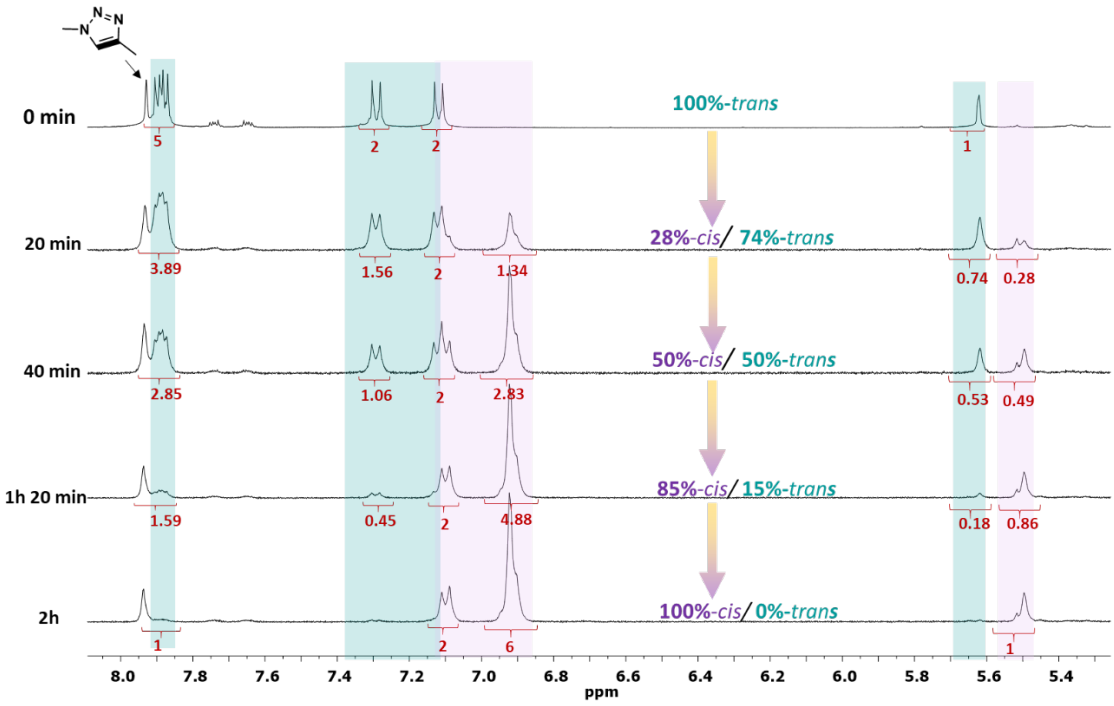

Figure S50. [1]HNMR photoisomerization *trans-cis* studies of compound **3** in MeOD.

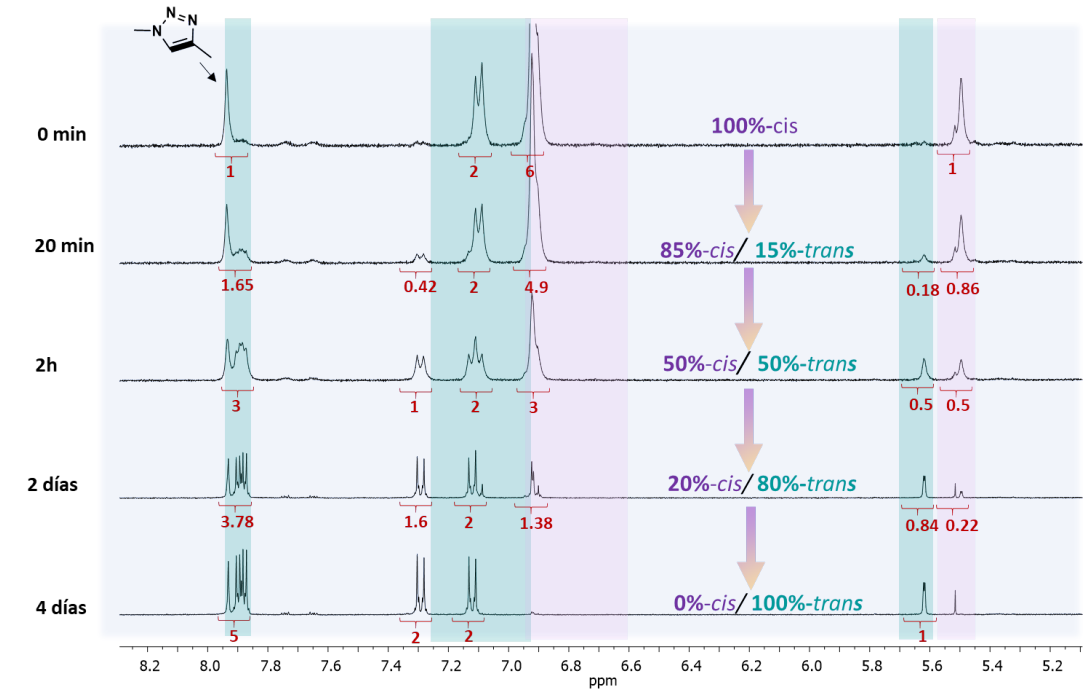

Figure S51. [1]HNMR study of reverse photoisomerization *cis-trans* in dark conditions of compound **3** in MeOD.

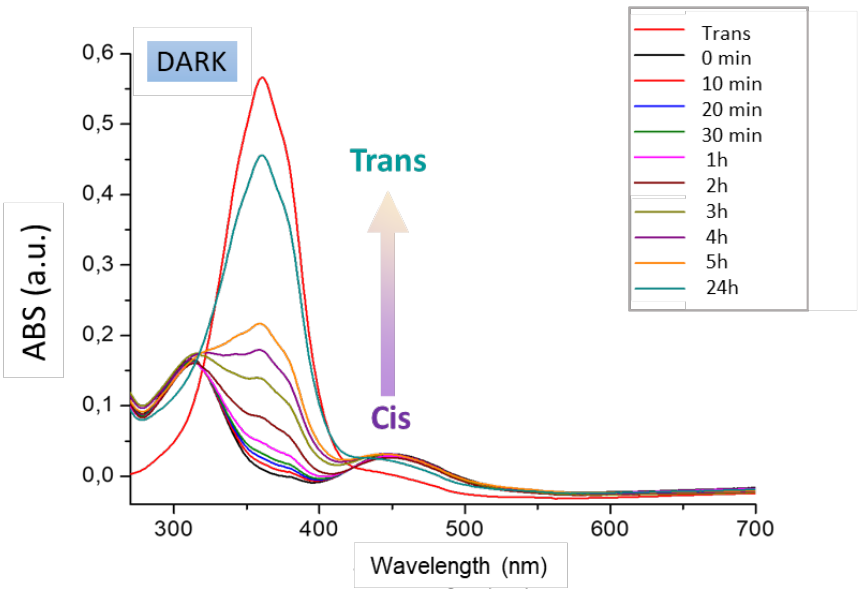

Figure S52. UV-Vis study of photoisomerization *cis-trans* in dark conditions of LNTs-**1** formed in 50% aqueous-ethanol.

6- 1D-SELECTIVE NOESY AND 2D EASY ROEY STUDIES

1D-NOESYand 2D 1H/1H EASY ROESY experiments were conducted with compound **2** cis using a mixture composed of 80% cis and 20% trans isomers. In the case of the 2-trans derivative, 1D NOESY experiments allowed a more precise assignments of aromatic signals, correlating them with their respective aromatic nuclei. Specifically, we detected NOE signals at 7.15 ppm when irradiating the methylene groups of the PEG chain at 4.205 ppm (Figure S53). This enabled us to confidently assign the doublet at 7.15 ppm to the H-3' and H-5' protons of the aromatic nucleus linked to the PEG chain.

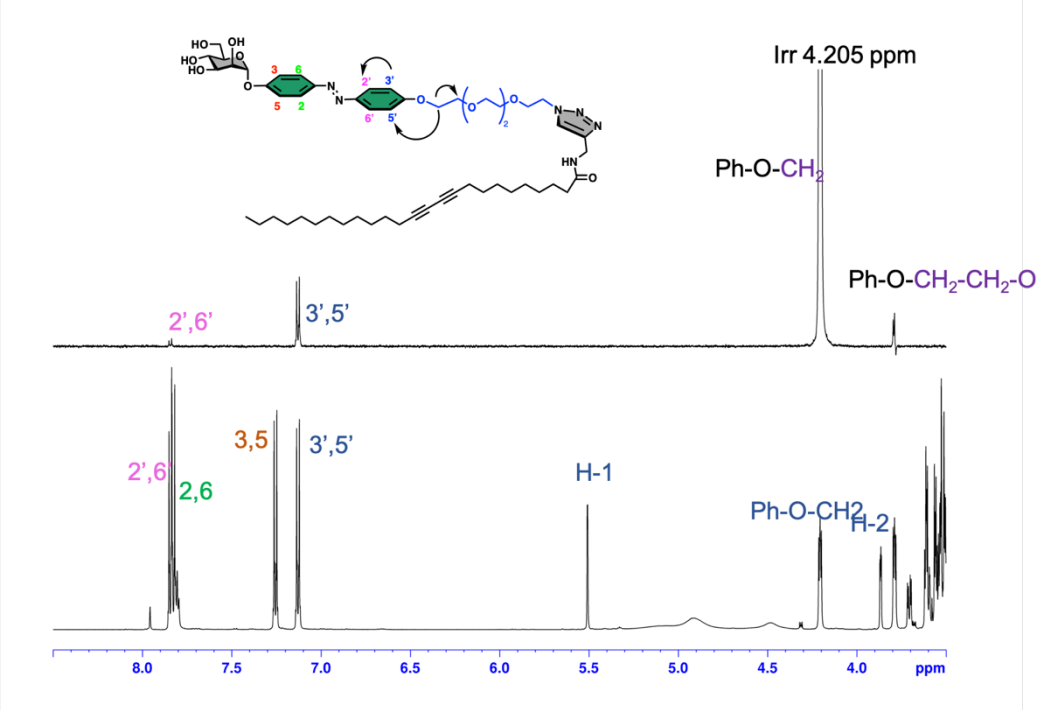

Figure S53. 1D NOESY (600 MHz, $DMSOd_6$) correlations for compound **2**-*trans*. Selective irradiation at 4.025 ppm (Ph-O-CH_2)

Similarly, we observed NOE signals at 7.25 ppm when irradiating the anomeric protons H-1 at 5.5 ppm, linking the doublet at 7.25 ppm to the H-3 and H-5 protons of the aromatic nucleus linked to the sugar.

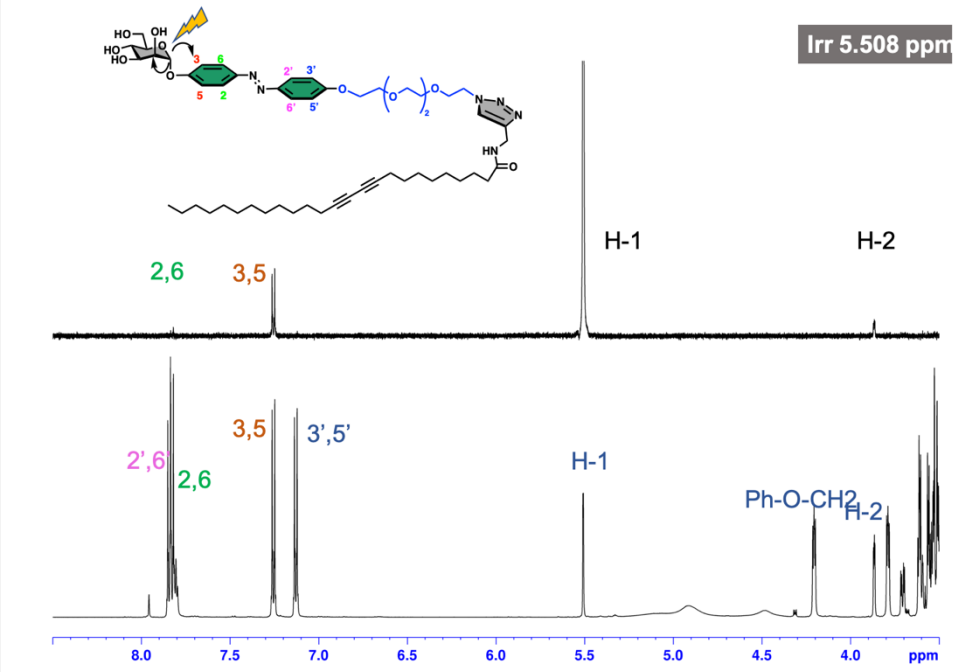

Figure S54. 1D NOESY (600 MHz, $DMSOd_6$) correlations for compound **2**-*trans*. Selective irradiation at 5.508 ppm (H-1, anomeric proton))

By conducting sequential irradiations of the doublets at 7.15 ppm and 7.25 ppm, we successfully assigned the corresponding signals to the H-2',6' and H2,6 protons, respectively, Figure.

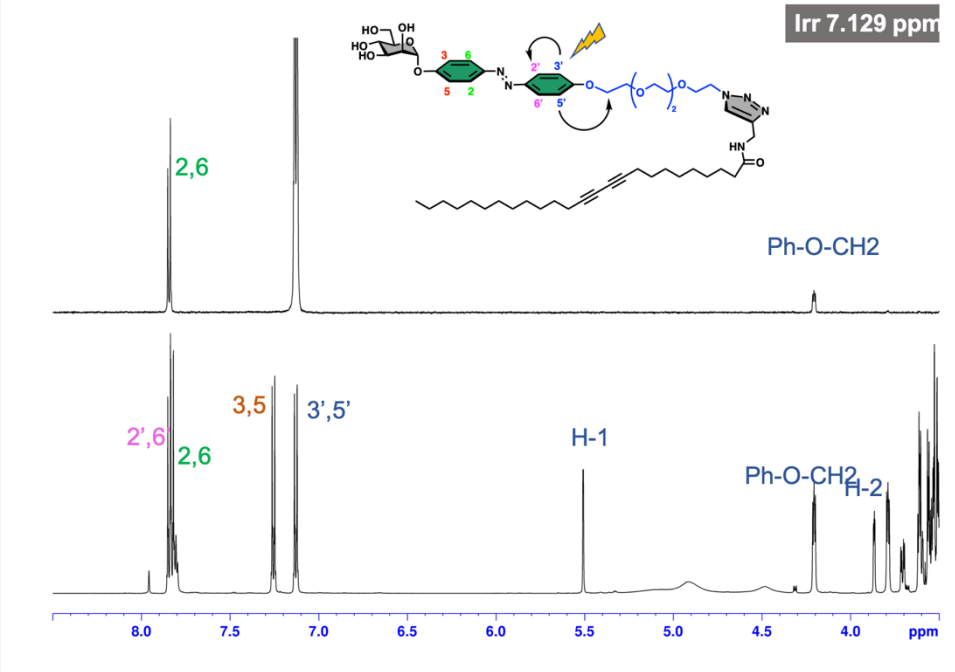

Figure S55. 1D NOESY (600 MHz, $DMSOd_6$) correlations for compound **2**-*trans*. Selective irradiation at 7.129 ppm (H3',5' of the aromatic ring)

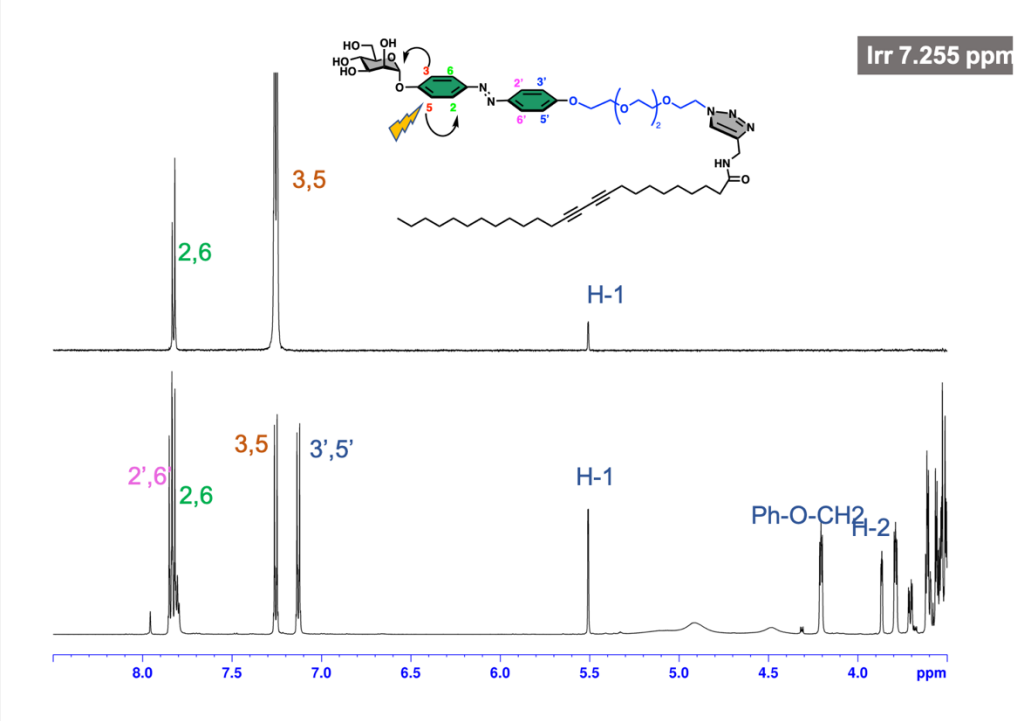

Figure S56. 1D NOESY (600 MHz, $DMSOd_6$) correlations for compound **2**-*trans*. Selective irradiation at 7.255 ppm (H3,5 of the aromatic ring)

For the **2-cis** derivative, the assignment proved to be more challenging due to the close chemical shifts of the aromatic protons in both rings. However, through the utilization of selective NOESY-1D experiments (figure S57 and S58), we managed to make the following assignments: the doublet at 7.03 ppm was correlated with the H3 and H5 protons of the aromatic nucleus linked to the sugar, the doublet at 6.83 ppm with the H2 and H6 protons, the doublet at 6.85 ppm with the H3',5' protons, and the doublet at 6.89 ppm with the H2',6' protons

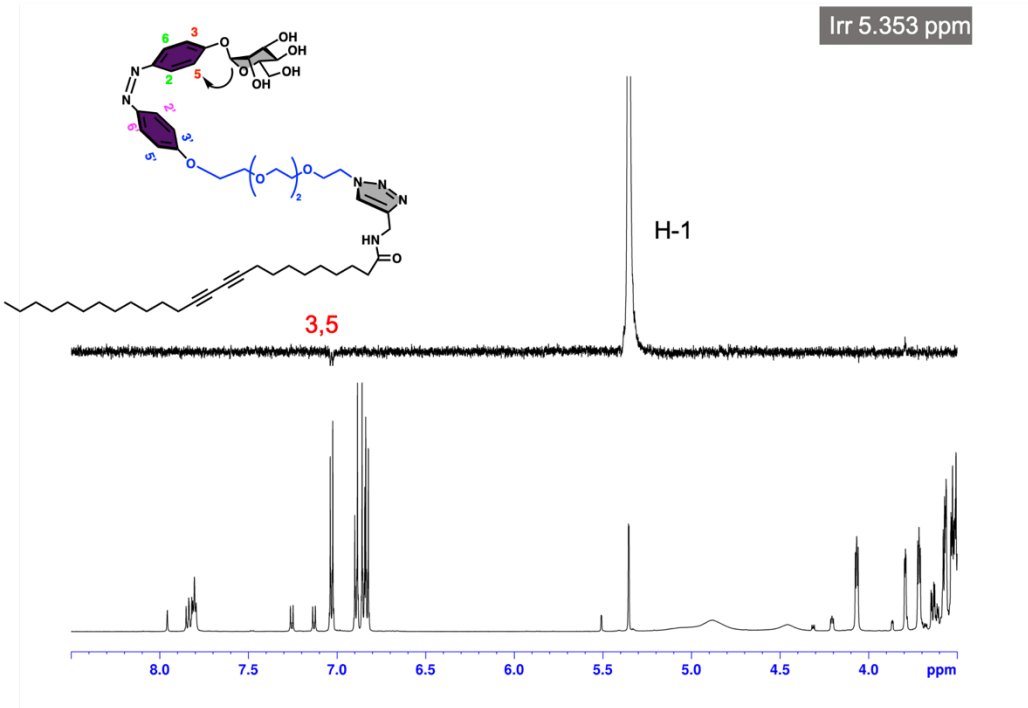

Figure S57. 1D NOESY (600 MHz, $DMSOd_6$) correlations for compound **2** (cis/trans; 80/20). Selective irradiation at 5.353 ppm (H-1, anomeric proton)

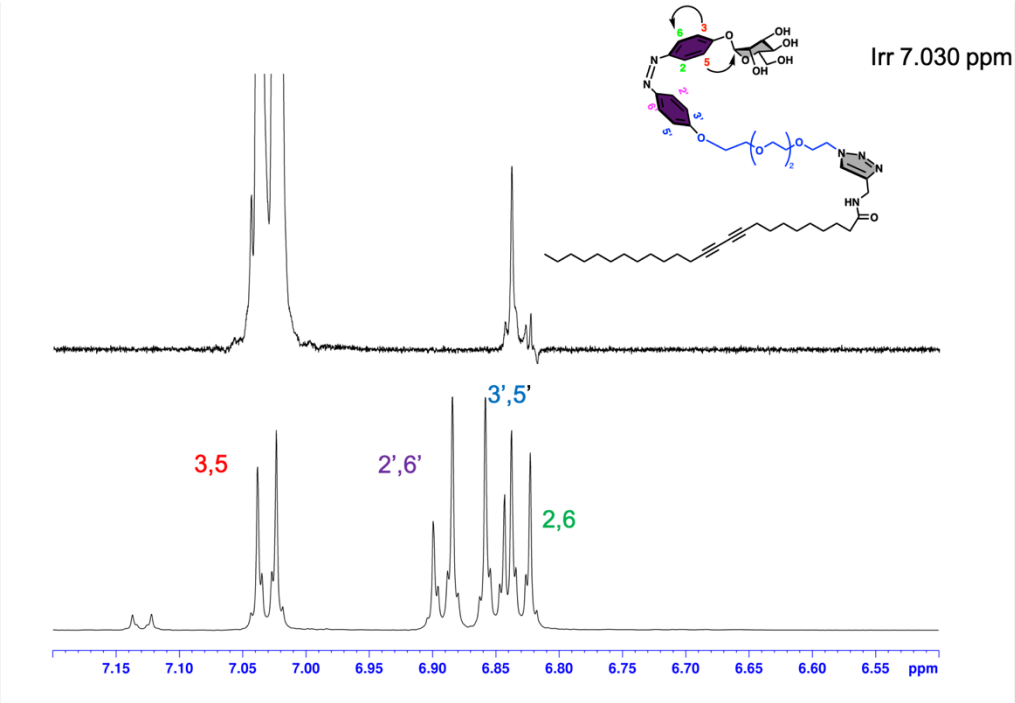

Figure S58. 1D NOESY (600 MHz, $DMSOd_6$) correlations for compound **2** (cis/trans; 80/20). Selective irradiation at 7.030 ppm (H3,5 of the aromatic ring)

Additionally, to explore potential additional contact points resulting from cis-isomerization, we conducted 2D 1H/1H EASY-ROESY experiments on the predominantly 2-cis mixture, Figure S59.

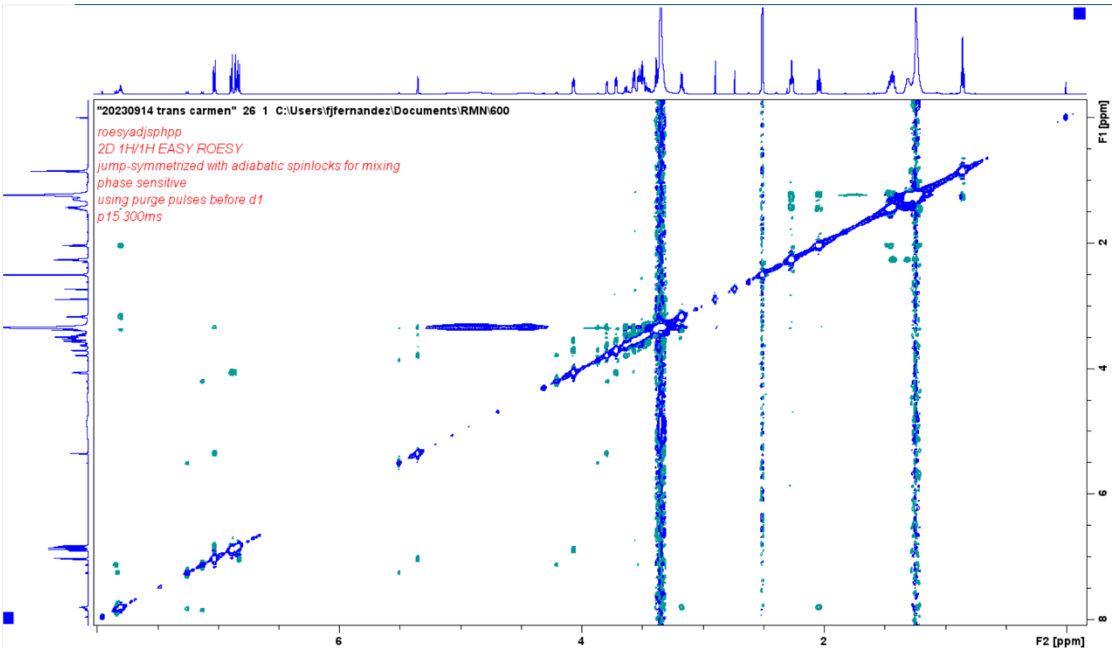

Figure S59. Full view of the 600 MHz 2D 1H/1H EASY ROESY NMR spectrum of a mixture of **2-cis/2-trans** (80/20) in $DMSOd_6$

These experiments not only reaffirmed our previous findings but also unveiled contact NOEs between the aromatic H3 and H5 protons and the CH_2 groups of the PEG chain, Figure S60.

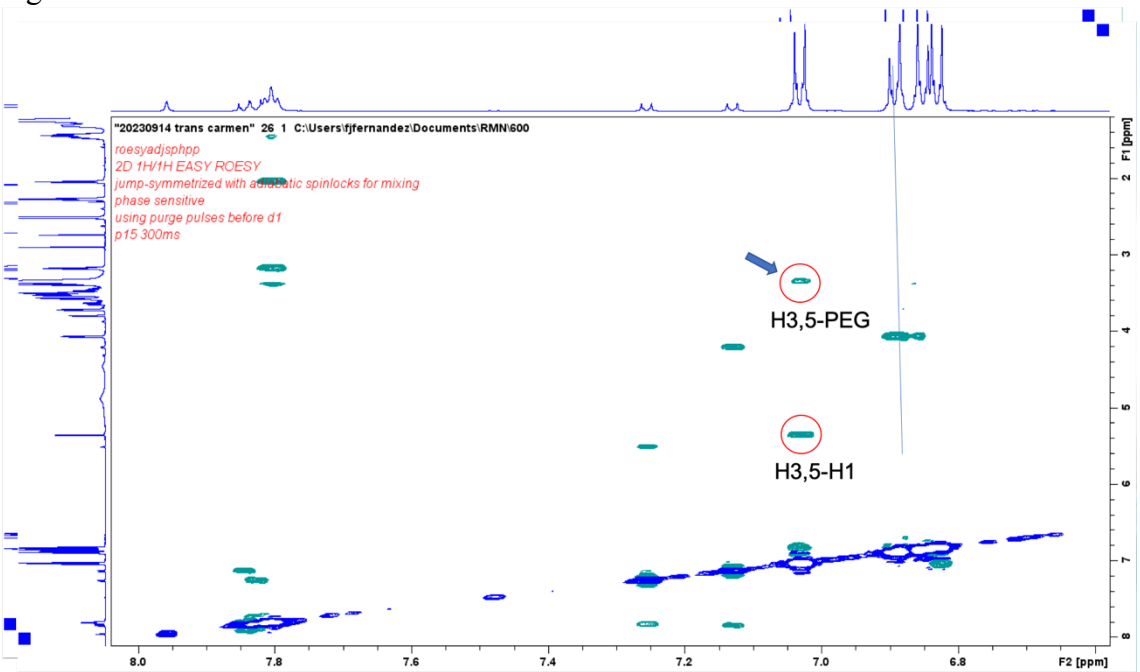

Figure S60. Partial view of the 600 MHz 2D 1H/1H EASY ROESY NMR spectrum of a mixture of **2-cis/2-trans** (80/20) in $DMSOd_6$ showing the noe between the H3,5 aromatic protons and the methylene protons of tetraethylene glycol spacer.

7- GELATION ABILITY STUDIES

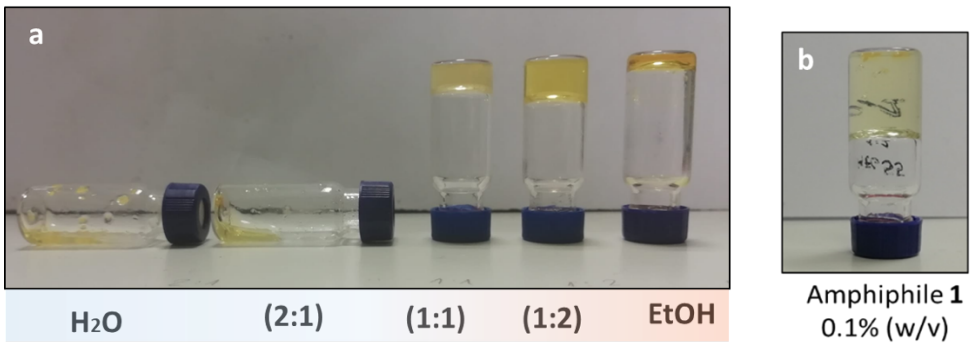

Figure S61: Photographs of vials showing the gelling abilities of amphiphile **1** in aqueous, aqueous-ethanol mixture and in pure ethanol (a), Photograph of vial showing the formation of glycogel from amphiphile **1** at 0.1% (w/v) in 50% aqueous ethanol (b)

8- SAXS Studies of the cis Hydrogel

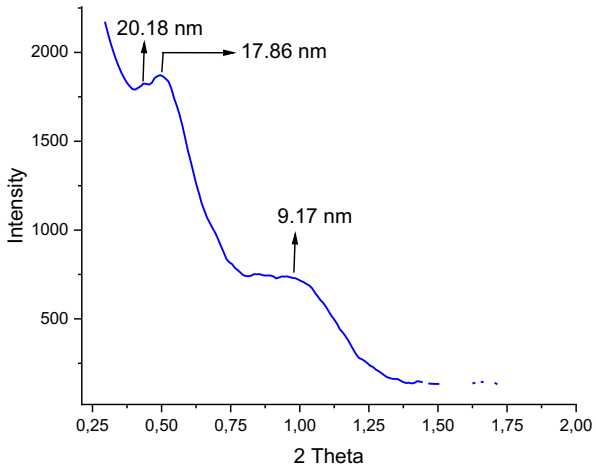

Figure S62. Small angle X-ray scattering of the cis **glycogel 1**

9- HPLC TRANS/CIS RATIO QUANTIFICATION OF 1 UNDER GELATION CONDITION

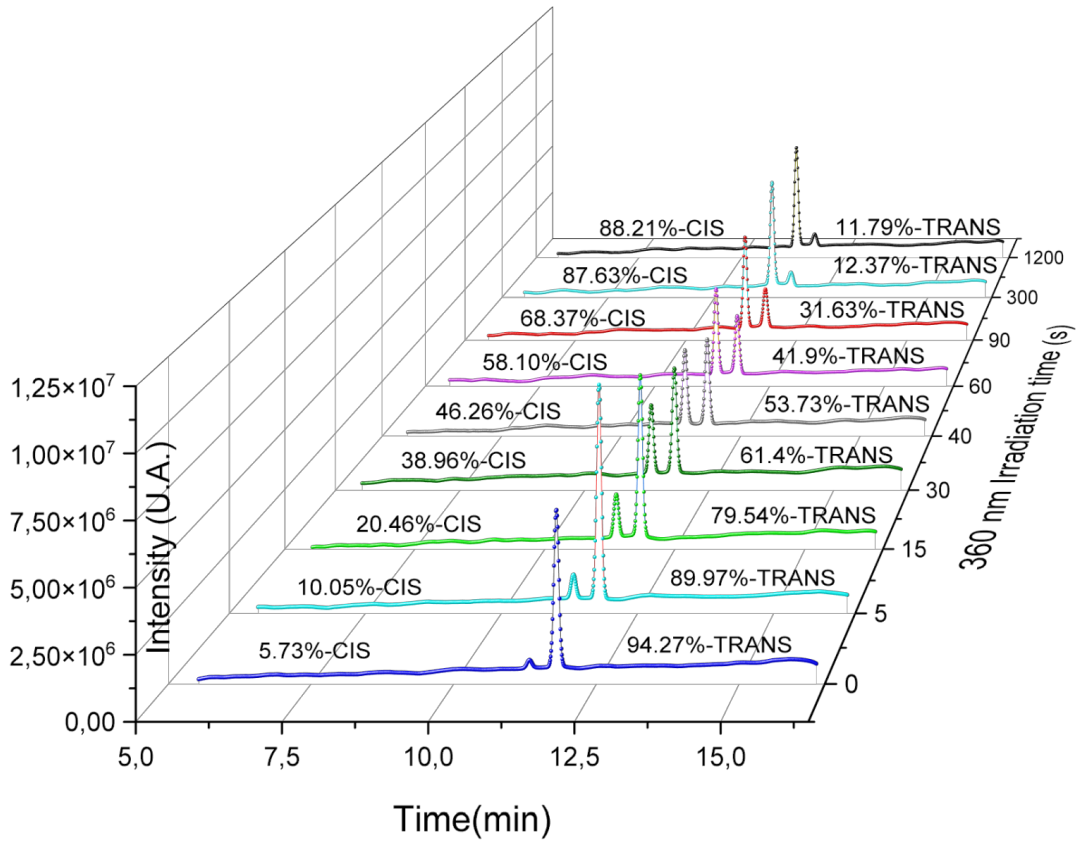

360 nm Irradiation Time (s)	Area (%; t=11.33 min)	Area (%; t=11.76 min)
0	5.73	94.27
5	10.03	89.97
15	20.46	79.54
30	38.96	61.4
40	46.26	53.73
60	58.10	41.9
90	68.37	31.63
300	87.63	12.37
1200	88.21	11.79

Figure S63. HPLC *trans/cis* isomerization and quantification through **360 nm** irradiation

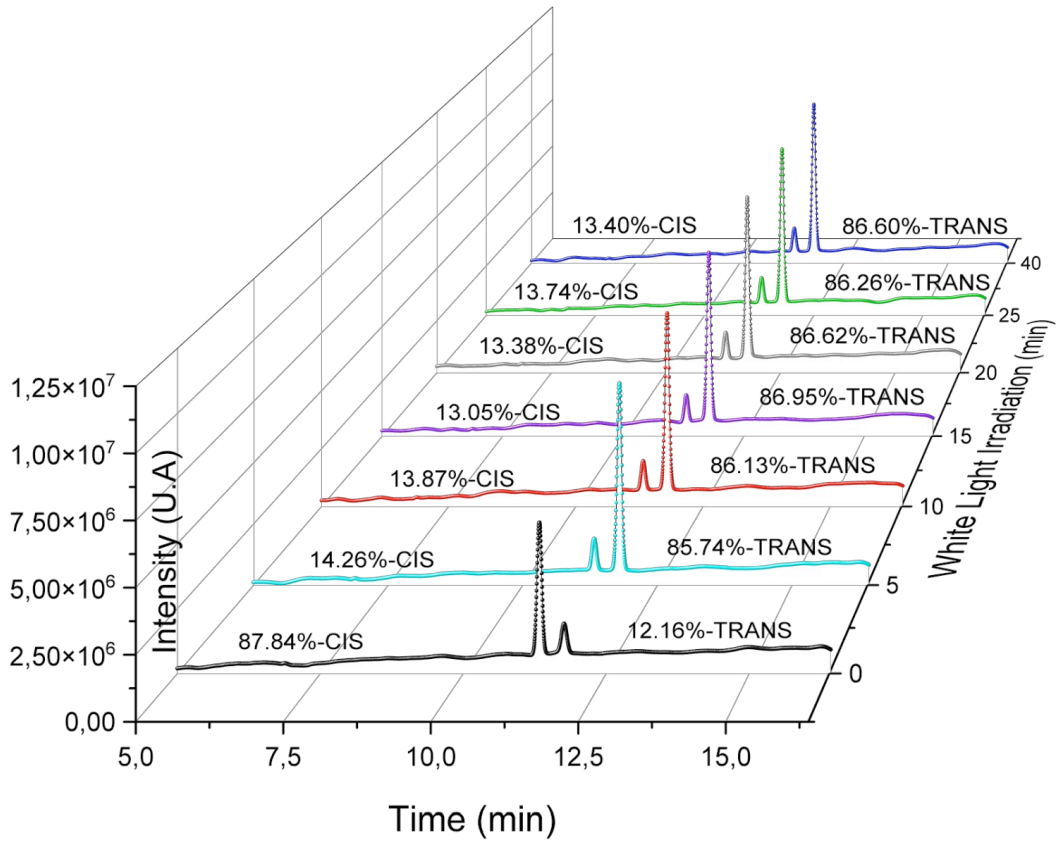

White Light irradiation time (min)	Area (%; t=11.33 min)	Area (%; t=11.76 min)
0	87.84	12.16
5	14.26	85.74
10	13.87	86.13
15	13.05	86.95
20	13.38	86.62
25	13.74	86.26
40	13.40	86.60

Figure S64. HPLC *cis/trans* isomerization and quantification through white light irradiation

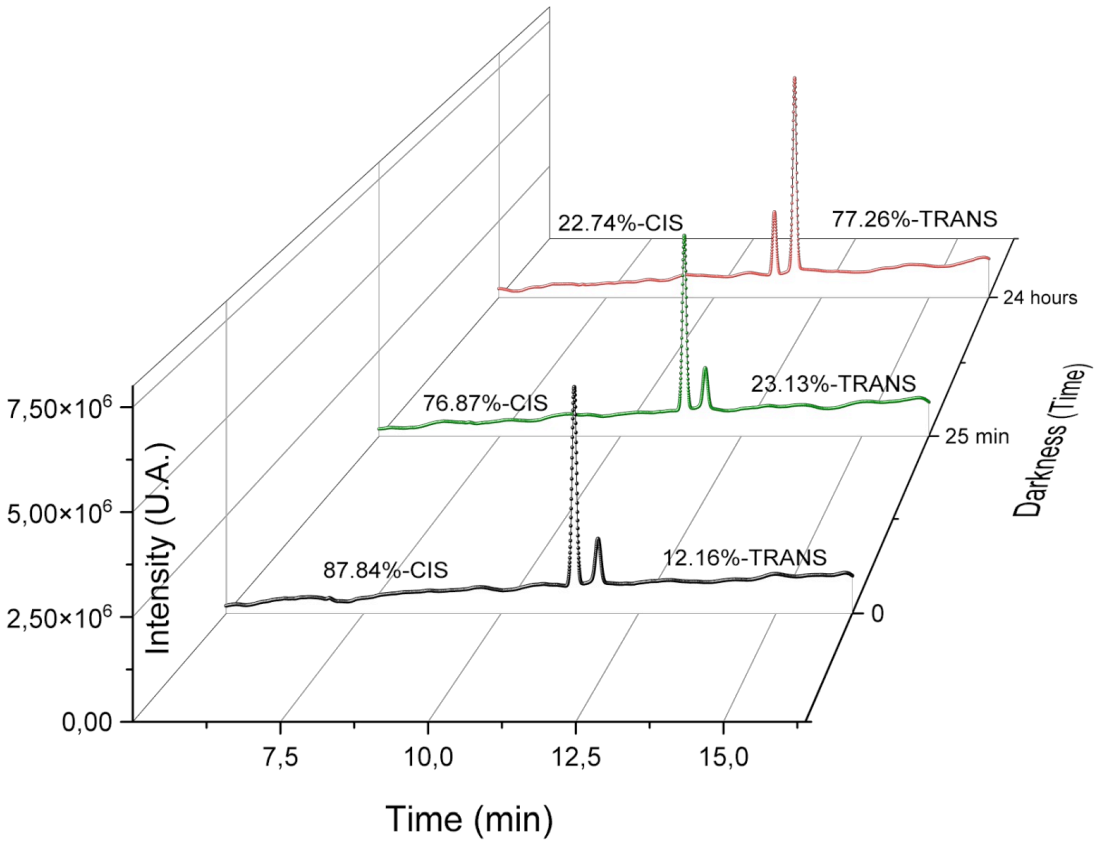

Darkness exposure	Area (%; t=11.33 min)	Area (%; t=11.76 min)
0	87.84	12.16
20 min	76.87	23.13
24 hours	22.74	77.26

Figure S65. HPLC trans/cis thermal isomerization and quantification in the dark

10- RELEASE ASSAYS

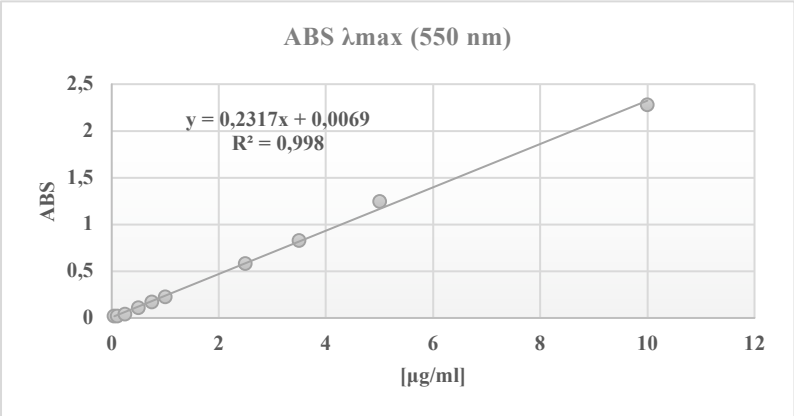

Figure S66. Calibration curve RhoB in (H2O/EtOH (1:1))

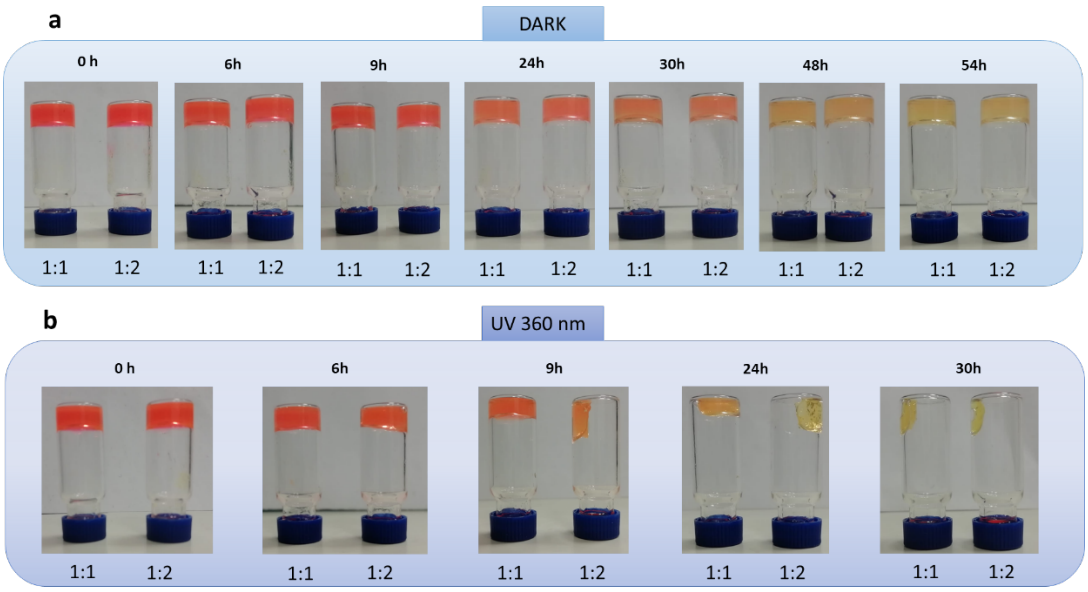

Figure S67: Photographs of the vials showing the release of rhodamine from glycogel **1** formed in 1:1 and 1:2 water-ethanol mixture: under dark conditions (a) and after 360 nm UV irradiation (b).

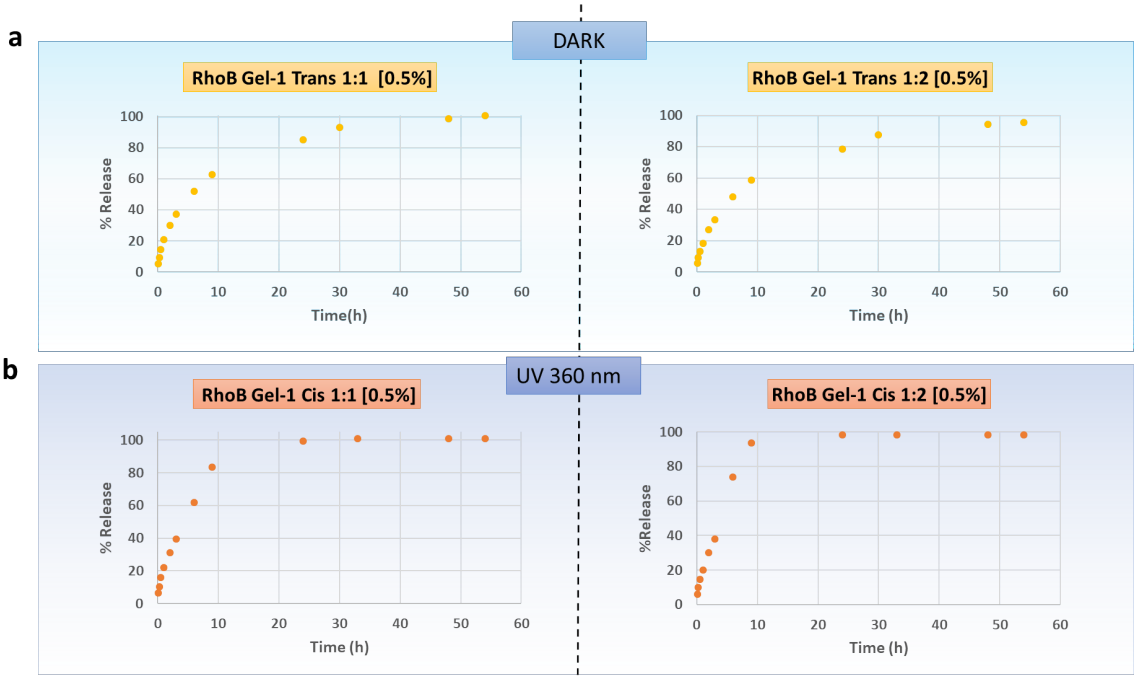

Figure S68. Release of Rhodamine B from Rho-containing glycogel **1** formed in 1:1 and 1:2 water-ethanol mixture: under dark conditions (a) and after 360 nm UV irradiation (b)

11- STUDIES ON THE PHOTOPOLYMERIZATION OF THE DIACETYLENIC MONOMER 1.

DA amphiphiles can be polymerized through a 1,4-addition reaction of diradicals produced by UV or γ irradiation, (Figure S69a),[1] affording polydiacetylene (PDA)-nanomaterials. In order for this topopolymerization to take place efficiently, the diyne monomer should be well-packed and arranged, ideally with a repeated distance of 5A°, typical for monomers in crystalline or liquid-crystalline state.[2,3] This polymerization which has been described in the case of films and vesicles, is easily eye-detected since PDAs acquire an intense blue coloration, consequence of conjugated ene-yne in the polymer backbone. In the case of the glycogel-1, however, no colour change was observed even after several hours of UV irradiation, indicating the absence or low degree of polymerization. This observation was confirmed by Raman studies, (Figures S69b and S69c). This behaviour, which has been observed previously in the case of other diacetylene-based nanostructures,[4] may be due to the imperfect alignment of the diacetylene groups in these nanostructures. In addition, the complex and three-dimensional nature of the gel, may difficult the uniform penetration of the UV light and thus complicate the polymerization in the gel state. However, in agreement with other reports,[5] by irradiating the glycogel-1 at the dry state the photopolymerization does take place as confirmed by the Raman spectrum. Indeed, unlike the spectrum obtained in gel state (Figure S69b), the Raman spectrum in the dry state (Figure S69c) shows the disappearance of the peak at 2268 cm−1 corresponding to the triple bond in the starting monomer and the appearance of two new peaks, one at 2084 cm^{-1} corresponding to the triple bond and the other at 1454 cm−1 that corresponding to the double bonds in the final PDA-1.[6]

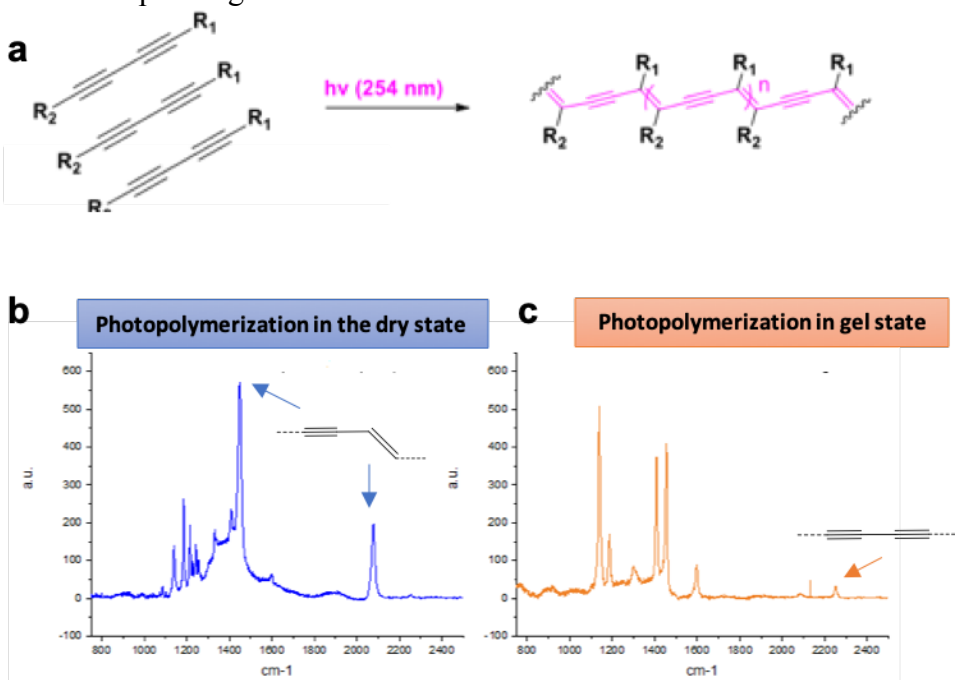

[1] G. Wegner, *Pure Appl. Chem.*, 1977, **49**, 443–454.

[2] C. Lim, D. J. Sandman and M. Sukwattanasinitt, *Macromolecules*, 2008, **41**, 675–681.

[3] A. V. Hall, O. M. Musa and J. W. Steed, *Cryst. Growth Des.*, 2021, **21**, 3614–3638.

[4] A. Perino, A. Klymchenko, A. Morere, E. Contal, A. Rameau, J. M. Guenet, Y. Mély and A. Wagner, *Macromol. Chem. Phys.*, 2011, **212**, 111–117.

[5] S. B. Lee, R. R. Koepsel and A. J. Russell, *Nano Lett.*, 2005, **5**, 2202–2206.

[6] Y. Wang, X. Chen, G. Zou and Q. Zhang, *Macromol. Chem. Phys.*, 2010, **211**, 888–896.

Figure S69. Schematic representation of UV-induced formation of polydiacetylene (PDA) from diacetylene monomers (a). Raman spectra at dry state (b) and at gel state (c)

12- STUDIES ON THE REOLOGICAL PROPERTIES OF GLYCOGEL-1.

The mechanical properties of **gel-1** were characterized by rheological strain sweep and frequency sweep experiments, (Figure S70). First, steady shear tests were carried out by logarithmically increasing the shear rate from 0.1 to 500 /s during 5 seconds, Figure 70a. Curves overlap very well demonstrating a very good reproducibility. The sample exhibited an astonishingly high low-shear viscosity that was expected in view of the apparent gel-like character of the samples. The sample also displays a shear-thinning behavior with a viscosity that strongly decreases with the shear rate (more than four orders of magnitude) as a result of the breakage of the physical bonds within the hydrogel. Finally, for very high shear rates (above 10^2-10^3) the viscosity levels off. At this stage, the inner microstructure is expected to be totally broken. To ascertain the mechanical hysteresis of the sample, the flow curve was also determined by sweeping the shear rate from 0.1 to 500 /s and back down to 0.1 /s, holding the shear rate fixed at each recorded point for 5 s, (Figure 70b). In view of Figure S70b, a hysteresis loop clearly appears. The fact that up-curves and down-curves do not collapse suggests that the sample may be thixotropic and that its rheological behavior is determined by the competition between microstructure build-up at rest and breakdown by flow. A similar observation has been reported for yield stress materials.[7] Dynamic oscillatory shear tests were also carried by logarithmically increasing the strain amplitude from 0.01 to 100 % at an excitation frequency of 1 Hz. Both storage (G') and loss (G'') moduli are shown as a function of the strain amplitude in Figure S70c.

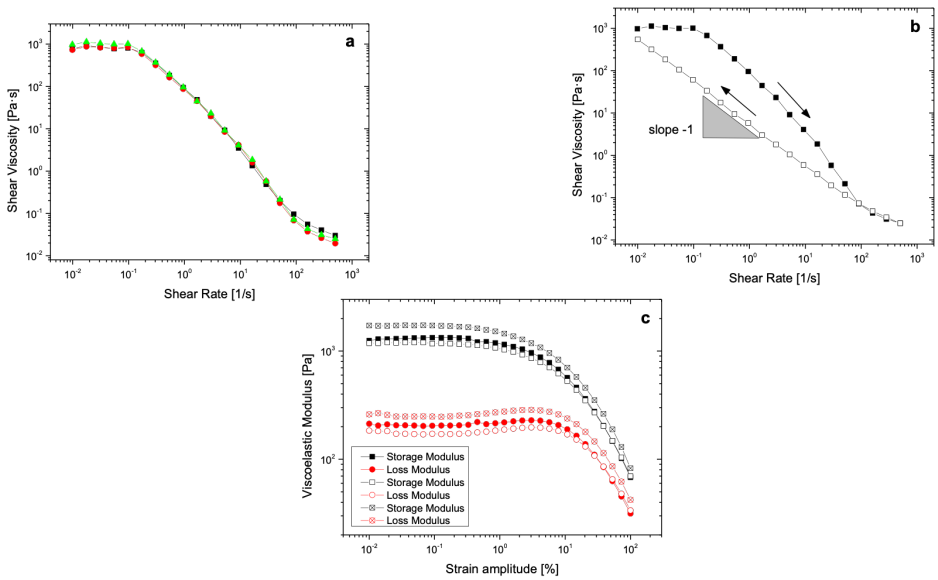

Figure S70. Steady shear viscosity as a function of the magnitude of the shear rate tensor (a). Viscosity curves under increasing (solid) and decreasing (open) shear rates (b). Viscoelastic moduli (G' and G'') as a function of the strain amplitude at a frequency of 1 Hz (c).

[7] D. Bonn, M. M. Denn, L. Berthier, T. Divoux and S. Manneville, *Rev. Mod. Phys.*, 2017, **89**, 1–40.

The sample behaves as a solid-like material with a G' that is nearly one order of magnitude larger than G'' in the full strain amplitude range investigated. The linear viscoelastic range extends up to a strain amplitude of 1 %. Above this strain level, non-linearities appear in the stress signal, the viscoelastic moduli start to decrease and the sample yields. For completeness, another set of dynamic oscillatory shear tests was carried out, to obtain the mechanical spectrum of the sample, by superimposing an oscillatory strain of amplitude 0.1 % and decreasing the excitation frequency from 10 Hz to 0.1 Hz. As expected for a gel-like material, the results (not shown here for brevity) showed a frequency-independent modulus.